HHS Public Access

Author manuscript

Mol Neurobiol. Author manuscript; available in PMC 2018 December 01.

Published in final edited form as:

Mol Neurobiol. 2017 December ; 54(10): 8287–8307. doi:10.1007/s12035-016-0262-z.

Lithium reversibly inhibits Schwann cell proliferation and differentiation without inducing myelin loss

Gonzalo Piñero[1,2], **Randall Berg**[1], **Natalia Andersen**[1], **Patricia Setton-Avruj**[2], and **Paula Monje**[1,*]

[1]The Miami Project to Cure Paralysis and the Department of Neurological Surgery, University of Miami Miller School of Medicine, Miami, Florida, United States of America.

[2]Universidad de Buenos Aires. CONICET. Instituto de Química y Fisicoquímica Biológicas (IQUIFIB). Buenos Aires, Argentina.

Abstract

This study was undertaken to examine the bioactivity, specificity and reversibility of lithium's action on the growth, survival, proliferation and differentiation of cultured Schwann cells (SCs). In isolated SCs, lithium promoted a state of cell cycle arrest that featured extensive cell enlargement and c-Jun downregulation in the absence of increased expression of myelin-associated markers. In addition, lithium effectively prevented mitogen-induced S-phase entry without impairing cell viability. When lithium was administered together with differentiating concentrations of cAMP analogs, a dramatic inhibition of the expression of the master regulator of myelination Krox-20 was observed. Likewise, lithium antagonized the cAMP-dependent expression of various myelin markers such as protein zero, periaxin and galactocerebroside and allowed SCs to maintain high levels of expression of immature SC markers even in the presence of high levels of cAMP and low levels of c-Jun. Most importantly, the inhibitory action of lithium on SC proliferation and differentiation was shown to be dose dependent, specific and reversible upon removal of lithium compounds. In SC-neuron cultures, lithium suppressed myelin sheath formation while preserving axonal integrity, SC-axon contact and basal lamina formation. Lithium was unique in its ability to prevent the onset of myelination without promoting myelin degradation or SC dedifferentiation. To conclude, our results underscored an unexpected antagonistic action of lithium on SC mitogenesis and myelin gene expression. We suggest that lithium represents an attractive pharmacological agent to safely and reversibly suppress the onset of SC proliferation, differentiation and myelination while maintaining the integrity of pre-existing myelinated fibers.

Keywords

Schwann cells; lithium chloride; myelination; dedifferentiation; cAMP; Krox-20

*To whom correspondence should be addressed: Paula V. Monje. Telephone: 305-243-8259; Fax: 305-243-3923; pmonje@miami.edu.

The authors declare that they have no conflicts of interest with the contents of this article.

Author contributions

G.P. and P.V.M. designed the study and wrote the manuscript; G.P., R.B, and N.D.A performed experiments; G.P., N.D.A, P.S. and P.V.M. analyzed and interpreted data. All authors read and approved the final manuscript.

Introduction

Lithium modulates a broad spectrum of cellular processes by means of interaction with diverse intracellular signaling systems in a manner similar to ligands that activate tyrosine kinase and G protein-coupled receptors. Lithium is a well-recognized direct inhibitor of the kinase activity of glycogen synthase kinase (GSK)-3β [1], which is a downstream effector within the signaling network driven by phosphatidylinositol-3-kinase (PI3-K) and protein kinase B or Akt. The interaction of lithium with these ubiquitous pathways has provided a molecular basis for its widespread role in stem cell lineage specification [2], proliferation [3] and differentiation in a variety of cell types [4,5].

In Schwann cells (SCs), the ensheathing and myelinating glial cells of the peripheral nervous system, the PI3-K pathway is a node of integration of signals emanating from the axons and the basal lamina, which collectively control the survival, proliferation and differentiation of SCs into myelin-forming cells [6]. SCs originate from multipotent neural crest cells that give rise to two well-defined stages during embryonic nerve development, the SC precursor and the immature SC [7]. In turn, these cells exit the cell cycle and differentiate into non-myelinating or myelinating cells as dictated by specific signals expressed in sensory or motor axons, respectively. In particular, isoforms of the ErbB/HER receptor agonist neuregulin (Neu) bound to the axonal surface promote SC proliferation [8], migration (motility), survival and myelination by triggering downstream signal transduction through the PI3-K/Akt pathway [9,10]. Extracellular matrix (ECM) components, including diverse isoforms of collagen and laminin located within the basal lamina, are also known to control SC proliferation and myelination through integrin receptor-dependent activation of PI3-K/Akt [11,12].

Lithium salts have been the conventional pharmacological treatment for bipolar and major depressive disorders for over six decades [13]. Additional benefits of lithium therapy include neuroprotective [14,15], anti-inflammatory [16] and anti-apoptotic effects [17], which have been exploited to treat central nervous system trauma [18,19] and chronic neurodegenerative diseases, such as Huntington’s disease, amyotrophic lateral sclerosis and Parkinson’s disease [20,21]. In the peripheral nervous system, it has been shown that lithium administration can foster functional recovery and re-myelination after injury [22,23]. Evidence from in vitro studies has been provided indicating that lithium enhances SC proliferation [24] and myelin gene expression [25,22].

In view of the clinical relevance and safety of lithium therapy for the treatment of nervous system diseases and its potential to mimic cellular responses dependent on PI3-K downstream signaling in mammalian cells [26], we sought to investigate the bioactivity, specificity and reversibility of lithium’s effects on primary SC cultures. To this end, we performed a comprehensive assessment of the action of lithium compounds on SC growth, survival, proliferation (S-phase entry), differentiation and myelin formation by using a variety of *in vitro* systems of stepwise complexity. Changes in cell function were monitored by a combination of live cell video-imaging microscopy, fluorescence microscopy, and western blotting. Contrary to our expectations based on previous reports, we found that lithium had a general counterbalancing action on the effect of growth factors known to

induce mitosis and myelination. A noticeable feature of lithium's action on SCs was its ability to promote cell enlargement and cell cycle arrest while maintaining SCs in a fairly undifferentiated state even in the presence of strong differentiating signals such as cyclic adenosine monophosphate (cAMP). Lithium halted proliferation and differentiation without driving SC dedifferentiation, compromising cell survival or altering the stability of myelinated fibers. In closing, the effects of lithium on cultured SCs were broad, highly specific, dose dependent and reversible upon lithium removal. These important features make lithium a promising pharmacological agent to safely modulate the rate of growth, proliferation and/or myelin formation of SCs during peripheral nerve development, injury or disease.

Materials and methods

Materials

Fetal bovine serum (FBS) was obtained from GE Healthcare Life Sciences (Pittsburg, PA). CPT-cAMP [8-(4-Chlorophenylthio) adenosine-3', 5'-cyclicmonophosphate] was procured from Calbiochem – EMD Millipore (Merck, Darmstadt, Germany). Recombinant human heregulin-β1 (herein referred to as neuregulin, Neu) was manufactured from Peprotech (Rocky Hill, NJ). Fluorodeoxyuridine (FudR), propidium iodide (PI), forskolin (Fsk), L-ascorbic acid, Sodium dodecyl sulfate (SDS), poly-L-lysine (PLL), mouse laminin from Engelbreth-Holm-Swarm murine sarcoma basement membrane, lithium chloride (LiCl), lithium carbonate (Li_2CO_3), potassium chloride (KCl) and sodium chloride (NaCl) were obtained from Sigma Aldrich (St. Louis, MO). CellTracker™ Green, DAPI (4',6-diamidino-2-phenylindole), Hoechst 33342 (herein referred to as Hoechst) and all secondary Alexa®-conjugated antibodies were acquired from Thermo Fisher (Waltham, MA). Antibodies against myelin basic protein (MBP, Cat. #. MAB386), myelin protein zero (P_0, Cat. #. AB9352), myelin-associated glycoprotein (MAG, Cat. #. MAB1567) and neurofilament (NF, Cat. #. AB5539) were purchased from Chemicon (Temecula, CA). Anti-c-Jun (Cat. #. sc-45), anti-β-catenin (Cat. #. sc-7963) and horseradish peroxidase (HRP)-conjugated secondary antibodies were obtained from Santa Cruz (Dallas, TX). Antibodies against glial fibrillary acidic protein (GFAP, Cat. #. Z0334) and S100 (Cat. #. Z0311) were obtained from DAKO (Carpinteria, CA). Anti-collagen type IV (Cat. #. 2150-1470) was from AbD Serotec-BioRad (Kidlington, United Kingdom). Antibodies against β-actin (Cat. #. D6A8), GSK-3β (Cat. #. 9332) and p-GSK3β (Serine-9, Cat. #. 9336) were obtained from Cell Signaling (Boston, MA). The O1 and O4 hybridoma cell lines were kindly provided by Dr. M. Schachner (Rutgers, Piscataway, NJ). The hybridoma cell lines for $p75^{NGFR}$ (clone 192) and Thy-1.1 were from the American Type Culture Collection (ATCC, Manassas, VA). Antibodies against Krox-20 and periaxin (Prx) were kind donations of Drs. Dies Meijer (University of Edinburgh, UK) and Peter Brophy (University of Edinburgh, UK), respectively.

Primary cultures of rat SCs

SCs were obtained from the sciatic nerves of adult (10–12 weeks old) female Sprague Dawley rats by a modification of a previously reported method [27]. Briefly, the sciatic nerve tissue was cut into small segments and allowed to degenerate *in vitro* by incubation for

10 days in High Glucose Dulbecco's modified Eagle Medium (DMEM) medium containing 10% heat-inactivated FBS (DMEM-10% FBS). Degenerated nerve explants were dissociated with a mixture of 0.25% Dispase II (Roche Diagnostics, Indianapolis, IN) and 0.05% type I collagenase (Worthington Biochemical Corporation, Columbus, OH) and the resulting cell suspensions were plated onto 10 cm dishes coated with PLL in DMEM-10% FBS. Contaminating fibroblasts were removed by a complement activation reaction (rabbit complement, MP Biomedicals, Santa Ana, CA) using Thy-1.1 antibodies present in the conditioned medium of Thy-1.1 hybridoma cultures. The purified SCs were expanded up to passage one in DMEM-10% FBS supplemented with 2 μM Fsk, 20 μg/ml bovine pituitary extract (Biomedical Tech., Stoughton, MA) and 2 nM Neu. Subsequent passages were carried out in DMEM-10% FBS supplemented with Fsk and Neu only using dishes sequentially coated with PLL and mouse laminin. Experimental conditions were tested using cultures consisting of >98% SCs based on double immunostaining with the SC-specific markers S100β and $p75^{NGFR}$. Experiments were routinely performed using SCs collected at passage 3–5. The percentage of contaminating Thy-1.1 positive cells was <2% regardless of the passage used. We have shown that expanded adult nerve-derived SCs obtained by this method do not differ significantly from early postnatal rat SCs [28] in their responses to cAMP and capacity to form myelin *in vitro* [29,30].

Fluorescent cell labeling

To achieve transient cell labeling, cells were labeled with the fluorescent vital dye CellTracker™ Green. Labeling was done according to the manufacturer's protocol 2–24 hours prior to visualization by live cell fluorescence microscopy. Briefly, adherent cells were washed twice to remove traces of serum prior to incubation (30 min, 37 °C, 5% CO_2) with CellTracker™ (6.5 μM) prepared in pre-warmed serum-free medium. This fluorescent dye is incorporated exclusively by living cells and retained for over 72 h without affecting cell viability. To achieve long-term fluorescent cell labeling, SC cultures were transduced at an early passage with a lentiviral vector encoding the green fluorescent protein (GFP), as described previously [31]. Transduction efficiency was typically >80%. Expression of GFP did not alter the viability, proliferation or differentiation of SC cultures.

Live cell video-imaging

Cells growing in 24-well plates were imaged by phase contrast microscopy using the IncuCyte ZOOM™ live cell imaging system (Essen BioScience, MI). Images of 16 non-overlapping fields per well were taken every 2 h using 20X objective lenses. Cells were video-imaged continually for a total period of up to 4–5 days from the onset of plating/treatment. Serial images of representative areas within individual spots were selected for display.

Cell viability assays

Cell viability was estimated by measuring the reduction of the tetrazolium compound [3-(4, 5-dimethyl-2-yl)-5-(3-carboxymethoxyphenyl)-2-(4-sulfophenyl)-2H-tetrazolium, MTS] into a soluble formazan compound, which displays an absorbance spectrum that peaks at 490 nm in presence of phenazine methosulfate. The reduction of the tetrazolium compound is dependent on the activity of cellular dehydrogenases, and thus represents a measure that is

directly proportional to the number of living cells and/or their metabolic activity [32]. Experiments were set up in PLL/laminin-coated 96-well plates containing cells plated at a density of 7,500 – 10,000 cells per well in DMEM-10% FBS. MTS assays were initiated by adding 20 μl of Cell Titer 96® AQueous One Solution Reagent per well in 100 μl culture medium followed by incubation for 3 h at 37 °C in a CO_2 incubator, according to the manufacturer's instructions (Promega, Madison, WI). Absorbance reading was carried out at 490 nm and 690 nm (corrective wavelength) using a microplate spectrophotometer plate reader (Bio-Teck, Winooski, VT) equipped with Gen5.0 Software.

Cell proliferation assays

The incorporation of [^{3}H]-thymidine or the thymidine analog EdU (Click-iT® EdU Alexa Fluor® 594 Imaging Kit, Thermo Fisher Scientific, Waltham, MA) into nuclear DNA was assayed as a measure of S-phase entry, as described previously [29]. SCs were plated in DMEM-10% FBS onto PLL/laminin-coated 24-well dishes (typically 60,000 – 80,000 cells/well). The medium was changed to HEPES-buffered DMEM containing 1% FBS (starvation medium) at least 1 day prior to being subjected to the different treatments. Cells were exposed to medium containing [^{3}H] thymidine (0.25 μCi/well) throughout the incubation period (typically 3 days) unless otherwise described in the figure legends. EdU labeling reagent was provided at 2 μM for 36 h prior to fixation. Cultures were assayed in triplicate samples in each experimental condition. Mitogenic concentrations of Neu (10 nM) and FBS (10%) were used for all stimulation experiments. Fsk (2 μM) was also added to the culture medium to allow for a synergistic (maximal) enhancement of proliferation [33]. The incorporated [^{3}H]-thymidine was determined by scintillation counting using a multi-purpose LS6500 Beckman Coulter (Brea, CA). EdU incorporation was determined by fluorescence microscopy in fixed cells. For this, the cells were fixed with 4% paraformaldehyde and processed for EdU detection according manufacturer's protocol. Additionally, nuclei were stained with Hoechst to reveal the total number of cells.

Differentiation and dedifferentiation assays

Isolated SCs were induced to acquire a differentiated phenotype by prolonged treatment with the membrane-permeable analog of cAMP, CPT-cAMP (herein referred to as cAMP), provided at 250 μM in DMEM-10% FBS in the absence or presence of lithium compounds. We have previously shown that cAMP effectively increases the expression of myelination-associated markers in the presence of serum factors [29]. To analyze lithium's effects on dedifferentiation, SCs were induced to differentiate with cAMP for 3 days prior to being subjected to treatment with lithium agonists in medium containing cAMP. Cultures maintained from the outset in the absence of cAMP-inducing agents served as a control for undifferentiated cells in both differentiation and dedifferentiation assays. Cells were analyzed for the expression of a wide range of SC- and myelin-specific markers by means of fluorescence microscopy and western blotting, as described below.

Cultures of dorsal root ganglion (DRG) neurons and myelin formation assays

Cultures of purified embryonic dissociated DRG neurons were established as described in previous publications [30]. The DRG bodies were dissected from rat embryos on the 15th day of gestation and then dissociated with 0.25% trypsin (37 °C, 45 min) followed by gentle

mechanical trituration. The resulting cell suspensions were plated as 30 μl drops containing 5,000 cells in the center of a culture well. This plating method renders cultures with the neuronal somas located roughly in the center of the well and the neurite outgrowth radiating outwardly towards the periphery of the well. Commercially available 24-well plates coated with poly-L-ornithine and laminin (BD Biosciences, San Jose, CA) were used to establish the neuronal cultures. Cultures were purified of non-neuronal cells by a 3-day treatment with the anti-mitotic agent FUdR (10 μM). The neuronal cultures were established and maintained in Neurobasal medium containing B27 supplement (Thermo Fisher Scientific, Waltham, MA), 25 ng/ml nerve growth factor (R&D Systems, Minneapolis, MN) and 1 mM L-glutamine (Thermo Fisher Scientific, Waltham, MA) up until the onset of myelination (see below). Typically, DRG neurons were used for experimentation within 10–20 days after culture initiation.

Myelinating co-cultures of SCs and DRG neurons were established essentially as previously described [34] with minor modifications [35]. SCs collected at passage 2–3 were dissociated with Trypsin/EDTA to obtain a single cell suspension, which was seeded on top of a network of purified dissociated DRG neurons. SCs were allowed to repopulate the axonal outgrowth (proliferation phase) for 7–10 days before inducing myelination by the addition of L-ascorbic acid (50 μg/ml) and 5% FBS (myelination phase) alone or together with lithium compounds, as indicated in the figure legends. Medium changes were performed on a 3-day basis up until cell fixation and analysis. This was carried out typically 7–10 days after initial ascorbate supplementation.

In order to analyze lithium's effect on myelin integrity, SCs were allowed to form myelin for 10 days prior to being subjected to treatment with LiCl for 2 days. Soluble Neu (provided at high concentration of 50 nM) was used as a positive control for preventing myelin formation and inducing myelin loss in myelinating SC-neuron cultures, essentially as described previously [36].

SC-neuron cultures were analyzed for the expression of SC- and neuron-specific markers, as follows: (1) co-immunostaining with O1 and MBP antibodies was used to identify myelinating SCs; and (2) immunostaining with O4 and collagen type IV antibodies was used to identify axon-related SCs and ECM components, respectively. Co-cultures were also routinely co-stained with antibodies against NF (axonal marker) and DAPI (nuclear marker), which served as reference controls for the extension of the axonal web and the location of the cells, respectively. To serve as negative controls, non-myelinating SC-neuron cultures were established and maintained in the absence of ascorbate supplementation throughout the time course of the experiments. SCs in ascorbate-deprived cultures typically lack the expression of markers of myelin (O1, MBP) and basal lamina (collagen IV).

Fluorescence microscopy and quantification of image data

Cultures were fixed for 20 min with 4% paraformaldehyde in PBS, followed by 10 min treatment with −20 °C methanol. Cultures were blocked in 5% normal goat serum in PBS; incubated overnight at 4 °C with primary antibodies in blocking solution (1:200–1:500) and then rinsed three times with PBS prior to incubation (1 h, room temperature) with Alexa®-conjugated (488, 546/594 and 647) secondary antibodies (1:300) and DAPI. Labeling of O1

and O4 antigens was done by incubating living cells with hybridoma culture supernatant (20 min, room temperature) before washing and fixing with 4% paraformaldehyde. Stained cultures were mounted with anti-bleaching mounting reagent consisting of 2.8% 1,4-Diazabicyclo[2.2.2]octane (DABCO, Sigma Aldrich, St. Louis, MO), 1% sodium azide in glycerol-PBS (9:1). Fluorescence microscopy analysis was performed using an Olympus IX70 inverted fluorescence microscope or a High Content Screening System (Cellomics ArrayScan VTI HCS Reader, Thermo-Scientific). Black and white images from fluorescence microscopy were artificially colorized, digitally processed, and arranged for presentation using Adobe Photoshop CS6 and Adobe Illustrator CS6. For cell quantification analysis, pictures from random fields were taken using 4-, 10- or 20X magnification objectives with numerical apertures of 0.13, 0.30, and 0.40, respectively. The number of cells labeled positive for the different markers was determined in reference to the total number of cells (DAPI/Hoechst staining of total nuclei). Cells were classified as positive or negative in reference to non-treated controls and disregarding the variability shown by individual cells

Quantification of the relative levels of O1, MBP and NF immunofluorescence in SC-neuron co-cultures was performed using Image J V1.48 (NIH, USA). Three independent measures were used to quantify the changes in myelination, as follows: (1) The integrated optic density (IOD) over a large surface area was used to estimate the overall (average) levels of O1, MBP and NF expression; (2) the proportion of myelinated (MBP/O1 positive) fibers/field was used to represent the local density of myelin segments regardless of their length and staining intensity; and (3) the length and thickness of MBP positive fibers was used to assess morphometric changes in individual myelinating cells. To calculate the IOD, fifty randomly selected fields (125x125 μm, 10x) from each replicate of each condition were used. IOD values were expressed in arbitrary units, and data for each marker was normalized to the IOD value obtained in the ascorbate condition, which was used as a reference control. The density of myelinated fibers was estimated by manual counting of the number of MBP positive and O1 positive myelin segments in randomly selected 10x fields located outside the area containing the neuronal somata. The length and thickness of MBP positive fibers was estimated based on individual measurements of perimeter and surface area as determined by individual object tracing and counting of particles using ImageJ.

Western Blots

Total cell lysates were prepared by re-suspending the cells in a buffer consisting of 50 mM Tris, 150mM NaCl, 1% SDS, and 0.5 mM dithiothreitol (DTT)-Cleland's Reagent (IBI Scientific, Peosta, IA) along with protease inhibitors (1 mM PMSF, 20 ng/ml aprotinin, and 20 μg/ml leupeptin, Sigma) and phosphatase inhibitors (phosphatase mixtures I and II, Sigma Aldrich, St. Louis, MO). Total proteins were quantified using Pierce™ 660nm Protein Assay Reagent (Thermo Fisher Scientific, Waltham, MA). Cell lysates were combined with SDS sample buffer (400 mM Tris/HCl, pH6.8, 10% SDS, 50% glycerol, 500 mM DTT, 2 μg/ml bromophenol blue) and denatures by 5 min of boiling. Equal protein samples (typically 1–5 μg /well) were subjected to polyacrylamide gel electrophoresis under denaturing conditions and transferred to polyvinylidene fluoride membranes (Millipore, Bedford, MA) by liquid transfer. Membranes were blocked with ECL blocking agent (Amersham Biosciences – GE Healthcare Life Sciences, Pittsburgh, PA) in Tris-buffered

saline containing 0.05% Tween 20 (TBS-T) and incubated overnight with the appropriate dilution of each primary antibody (typically 1:1,000–1:2,000). The membranes were washed three times with TBS-T prior to incubation with HRP-conjugated secondary antibodies (1:5,000 to 1:10,000). Immunoreactivity protein bands were detected by enhanced chemiluminescence (ECL) using ECL Plus according to the manufacturer's instructions (GE Healthcare Life Sciences, Pittsburgh, PA). To determine the relative changes in the levels of expression of cell surface O1, live SCs cultures were incubated with O1 or O4 antibodies and washed extensively before preparing the cell lysates used in electrophoresis. Anti-O1/O4 immunoglobulins were detected by ECL after incubating the membranes with anti-mouse-HRP. Whenever appropriate, the unchanged expression of β-actin is shown as a control of equal cellular protein loading. The total levels of expression of GSK3 and ErbB3, a SC-specific marker, also served for normalization.

Statistical analysis

The results provided in the figures are representative of at least 3 independent experiments performed using different batches of cells. Quantitative data is presented as the mean ±SEM obtained from triplicate samples, unless otherwise described in the figure legends. Statistical analysis was performed using GraphPad Prism version 5.00 (GraphPad Software, San Diego, CA). Data regarding tests, post-tests and statistical significance is indicated in the figure legends.

Results

Lithium induces extensive morphological changes without increasing the expression of myelin-associated markers in isolated primary SCs

To begin analyzing lithium's effects on SC proliferation and differentiation, we treated primary rodent SCs with the widely used formulation lithium chloride (LiCl) and used IncuCyte ZOOM™ live cell video-imaging technology to record the changes in cell density and morphology over a period of up to 4 days. As shown in the selected phase contrast images provided in Figure 1a, LiCl promoted dynamic changes in SC morphology that were noticeable early after plating but became more prominent with prolonged exposure to the LiCl stimulus. These images clearly revealed that LiCl-treated SCs failed to both extend processes and acquire the characteristic bipolar shape shown in control cells (Fig. 1a, left panels). In the presence of LiCl, SCs remained highly viable but progressively attained a flattened, expanded morphology with a roughly enlarged nucleus and intracellular vacuoles (Fig. 1a, middle panels). Curiously, changes in cell shape and size induced by LiCl resembled those driven by treatment with cell permeable analogs of cAMP, which are known to provide a strong differentiating stimulus for SCs via inducing cell cycle exit and myelin gene expression [37,29]. Therefore, to more closely compare the temporal progression of changes in LiCl-treated and cAMP-treated SCs, respectively, selected images of SC cultures induced to differentiate in response to cAMP [29] were also included in the analysis (Fig. 1a, right panels).

Next, to obtain a higher resolution view of the morphological transformation, SC cultures were treated as above and stained with the vital dye CellTracker™ Green prior to

visualization by live cell fluorescence microscopy. Fluorescent cell labeling analysis revealed that similar to cAMP, LiCl induced a widespread extension of the cell membrane along with the appearance of intracellular vacuoles (Fig. 1b). Results from western blot analysis indicated that LiCl suppressed the expression of the transcription factor c-Jun/AP1 resembling the pro-differentiating action of cAMP (Fig. 1d), [38,31]. Nevertheless, further analysis by immunofluorescence microscopy and western blot revealed that these changes occurred without a concurrent induction of the expression of key markers of differentiation such as Krox-20, MAG, Prx, P_0 and galactocerebroside,O1, (Fig. 1c–d). Contrary to cAMP treatment, the levels of expression of immature SC markers such as GFAP and $p75^{NGFR}$ [39,29] did not change in LiCl-stimulated SCs (Fig. 1d, shown only for GFAP). A minor increase in the expression of the pre-differentiation marker O4 (cell surface sulfatide) was observed upon prolonged exposure to the LiCl stimuli. Still, the magnitude of O4 expression was significantly lower than that driven by cAMP (Fig. 1c).

The bioactivity of LiCl's action in SCs was confirmed by western blot analysis of GSK-3β phosphorylation on Serine-9, an inhibitory site on GSK-3β that is specifically phosphorylated by the upstream kinase Akt (Fig. 1d–e), [1]. The effect of LiCl on GSK-3β phosphorylation was highly dependent on the dose of LiCl used and the time of administration (Fig. 1e). As expected, the increased phosphorylation of GSK-3β induced by LiCl closely correlated with an increased expression of β-catenin (Fig. 1e), a direct downstream target of the kinase activity of GSK-3β that is stabilized and accumulated in the cytoplasm upon GSK-3β inactivation.

In sum, these results illustrated the prominent role of lithium compounds on initiating signal transduction in SCs in connection to inducing extensive morphological changes and disappearance of c-Jun in the absence of increased expression of myelin-specific markers.

Lithium specifically and reversibly inhibits mitogen-induced S-phase entry while preserving cell viability

To understand the functional consequences of the striking morphological changes induced by lithium, we examined the effect of LiCl in SCs growing under conditions supportive of active proliferation. For this, we performed live cell video-imaging experiments in isolated SCs treated with LiCl in medium supplemented with a combination of soluble Neu peptide (an ErbB/HER agonist) and Fsk (a direct adenylyl cyclase activator), as this media formulation is capable of inducing maximal levels of proliferation [33]. Results indicated that LiCl not only prevented the mitogen-induced increase in cell density but also induced a dramatic morphological transformation of the cells despite the presence of Neu and Fsk (Fig. 2a). As expected, treatment with an equimolar dose of NaCl, which was used as a specificity control, had no apparent effect on the morphology or the density of cells (Fig. 2a). To validate these results, we next tested whether LiCl had a detrimental effect on the overall health of the cells. This was accomplished by assessing the viability of the cultures in Neu/Fsk-supplemented medium using a combination of MTS assays and propidium iodide (PI) incorporation assays (Fig. 2b–c). Whereas the former assays provide a biochemical measure of total dehydrogenase activity in metabolically active cells, the latter assays provide a relative measure of cell death as PI is only incorporated into the nuclei of dead

cells. In close correlation with the reduced cell density (Fig. 2a), the levels of dehydrogenase activity under conditions supportive of mitogenesis were markedly reduced in the presence of LiCl but not NaCl (Fig. 2b). We confirmed that this was not due to cell death based on data showing an unchanged proportion of PI positive cells in LiCl-treated cultures with respect to control (Fig. 2c). Of note, LiCl did not change the basal levels of dehydrogenase activity and PI incorporation at any of the concentrations tested under non-mitogenic conditions (not shown).

One specific feature of the SC's responses to LiCl stimulation was the conspicuous phenotypic transformation induced by prolonged lithium treatment possibly linked to cell cycle arrest (Figs. 1a–b and 2a). To test the reversibility of the LiCl-driven changes in cell morphology, we subjected SCs to repeated cycles of LiCl addition and removal prior to analysis by fluorescence microscopy (Fig. 2d). To monitor the cells over a prolonged period of time, experiments were performed using lentivirally infected SCs transduced to express the green fluorescent protein (GFP). GFP-SCs were treated every 3 days with culture medium containing LiCl (+ LiCl, 30 mM) or vehicle (−LiCl, control) and pictures of live GFP fluorescence were obtained regularly, essentially following the schedule presented in Fig 2d (graphical bars). Representative images of LiCl-treated (+LiCl) and LiCl-deprived (−LiCl) cultures taken at 3-day intervals over a time course of 9 days following the onset of treatment revealed the fast recovery of an elongated, bipolar morphology after the removal of the LiCl stimulus (Fig. 2d). Typically, a 3-day period of re-exposure to LiCl was sufficient for SCs to regain an enlarged, expanded shape. Acquisition of an elongated shape was not observed in cultures receiving re-addition of LiCl either in the absence (not shown) or presence (Fig. 2d) of serum or soluble mitogenic factors.

Another specific feature of LiCl's action in SCs was its ability to prevent expansion of the cell population (Fig. 2a). Thus, we subsequently carried out EdU and [^{3}H]-thymidine incorporation assays to confirm whether lithium would exert a direct inhibitory action on mitogen-induced S-phase entry. As shown in Figure 3a–b, the addition of LiCl (but not NaCl) reduced the proportion of cells that incorporated the EdU label into nuclear DNA to nearly basal levels. LiCl strongly and specifically reduced EdU incorporation when administered in the presence of serum alone (weak proliferative stimulus), Supplementary Fig.a–b, or together with Neu and Fsk (maximal proliferation), Fig. 3a–b. In addition, LiCl reduced DNA synthesis in a dose-dependent (Fig. 3c), lithium-specific (Fig. 3d) and reversible manner (Fig. 3e). The requirement of lithium was reflected by the fact that an equimolar concentration of Li_2CO_3 inhibited whereas NaCl or KCl had no effect on S-phase entry, as determined by scintillation counting of incorporated [^{3}H]-thymidine (Fig. 3a–b and d). The reversibility of lithium's action was indicated by the high levels of [^{3}H]-thymidine that SCs incorporate after the withdrawal of LiCl from the culture medium (Fig. 3e). LiCl withdrawal allowed SCs not only to regain their typical elongated, bipolar shape (Fig. 2c) but also effectively re-enter the cell cycle in response to soluble mitogenic factors (Fig. 3e, right bar).

To summarize the above results, lithium specifically, reversibly and dose dependently inhibited cell cycle progression in isolated SCs without compromising cell survival. By contrast to previous reports [24], we found that lithium effectively counteracted the pro-

mitogenic effects of serum, Neu and Fsk and arrested SCs in the cell cycle without changing the expression myelin-specific markers.

Lithium effectively counteracts the pro-differentiating action of cAMP

The ability of lithium to promote cell enlargement along with cell cycle arrest motivated us to further investigate whether lithium could enhance SC differentiation into myelin-forming cells, as cell cycle exit is an important pre-requisite for the onset of myelin gene expression [40,41]. To begin addressing this question, we performed experiments in SC-only cultures that consisted essentially of inducing differentiation by provision of cell permeable analogs of cAMP in the absence or presence of pharmacological lithium compounds [29]. For this, the changes in cell shape along with the expression of markers typical of mature (myelinating) and immature SCs were monitored over time using a combination of live cell video-imaging, fluorescent microscopy and western blot analysis. Time lapse microscopy indicated that LiCl-treated SCs failed to undergo the typical morphological transformation that occurs in response to prolonged cAMP stimulation (data not shown). In addition, results from immunofluorescence microscopy and western blot experiments revealed that the cAMP-induced expression of the myelin-specific galactolipid O1 and the early transcriptional enhancer of myelination Krox-20 were effectively and dose dependently reduced in the presence of LiCl (Fig. 4a–d). Western blot detection of a broader panel of myelin proteins, including P_0 and Prx confirmed lithium's potency to prevent the cAMP-dependent expression of myelinating SC markers (Fig. 4b). Interestingly, LiCl-treated cells maintained their characteristic spindle-shaped morphology even in the presence of cAMP. This was evidenced by co-immunolocalization of O1, and S100, a cytoplasmic SC-specific marker (Fig. 4a).

Additional immunostaining and western blot experiments suggested that LiCl exerted an antagonistic action on the cAMP-dependent reduction of immature SC markers such as GFAP (Fig. 5a–c) and $p75^{NGFR}$ (Fig. 5b). Results indicated that LiCl-treated cultures were essentially undistinguishable from untreated controls on the basis of the expression of the abovementioned immature SC markers with the exception of c-Jun, which is a transcriptional inhibitor of peripheral myelination [38]. Curiously, LiCl dramatically reduced the levels of expression of c-Jun either in the absence or presence of cAMP and it did so irrespective of changes in other immature SC markers (Fig. 5a–c). Evidence is provided showing maintenance of high levels of expression of two markers typical of immature/mature SCs, S100 (Fig. 5a) and O4 (Fig. 6b), in lithium-treated SCs [39]. Of note, higher doses of LiCl reduced P_0 expression in both control and cAMP-stimulated SCs (Fig. 4b and 5c).

Altogether, it seems apparent that lithium can inhibit the cAMP-dependent expression of Krox-20 and other myelin markers while maintaining high levels of immature SC markers. This occurred even in the presence of differentiating concentrations of cAMP and virtually no c-Jun expression.

Lithium antagonizes cAMP-driven differentiation in a reversible and specific manner

The potent inhibitory effect of LiCl on cAMP-induced SC differentiation was an unexpected observation based on reported studies suggesting a positive action of lithium on the expression of MAG, P_0 and PMP22 [25,22]. Thus, we performed a series of experiments to test both the specificity and reversibility of lithium's antagonism on cAMP-driven differentiation in SC cultures treated with LiCl, Li_2CO_3 and other chloride compounds. Experiments presented in Fig. 6 indicated that lithium's antagonism on cAMP-induced differentiation was lithium-specific. Firstly, the inhibitory action of LiCl on the cAMP-driven expression of O1 (Fig.6a), Krox-20, and P_0 (Fig. 6b, left panels) was mimicked by an equimolar dose of Li_2CO_3. Secondly, neither NaCl nor KCl were sufficient to change the expression of these markers in the way shown by chemical lithium compounds (Fig. 6a right panels and 6c). Li_2CO_3 rather than NaCl or KCl allowed SCs to maintain a bipolar phenotype (Fig. 6a, S100 expression) and high levels of GFAP (Fig. 6b) despite prolonged CPT-cAMP administration.

Experiments presented in Fig. 7 indicated that the anti-differentiating action of lithium was reversible upon lithium withdrawal from the culture medium. Reversibility experiments consisted on subjecting SCs to a 3-day pre-treatment with 30 mM LiCl or vehicle (control) prior to addition of cAMP in lithium-free medium. Results indicated that cAMP failed to increase the expression of O1 (Fig. 7a), Krox-20 and P_0 (Fig. 7b) in LiCl-containing rather than LiCl-free medium, regardless of previous exposure to LiCl stimulation. The action of cAMP on the expression of these markers was readily restored once LiCl was removed. Lithium removal allowed SCs to respond to the cAMP stimulus by increasing the levels of Krox-20, O1 and P_0 (Fig. 7a), as well as downregulating the levels of GFAP (Fig. 7b). Staining with S100 antibodies (Fig. 7a) also revealed that removal of LiCl was sufficient to allow cAMP-treated SCs to shift their phenotype from an elongated, bipolar shape to an enlarged, fattened one.

To conclude, the evidence provided herein supports the high specificity and reversibility of lithium's inhibitory action on cAMP-driven SC differentiation. Surprisingly, LiCl elimination was sufficient to restore all typical differentiating responses to cAMP in isolated SCs.

Lithium interferes with the maintenance of Krox-20 expression without promoting SC dedifferentiation

A prominent feature of lithium's action was its strong inhibitory effect on Krox-20 expression. Downregulation of Krox-20 is a typical feature of the SC's responses to nerve injury and other signals inducing SC dedifferentiation into a less mature state [41]. Loss of Krox-20 expression has been shown to occur in concert with an increase in the expression of immature SC genes, such as c-Jun and GFAP, along with cell cycle re-entry [41]. To more specifically address whether lithium could halt Krox-20 expression in mature (Krox-20 positive) cells and/or induce a reversal of the differentiated state, we performed experiments that consisted of delaying the provision of LiCl with respect to the addition of cAMP prior to assessing the expression of differentiation markers (Fig. 8). In some experiments (Fig. 8a–d), the effect of LiCl was compared to that of an equimolar dose of NaCl, which was used to

control the specificity of lithium's action. In other experiments (Fig. 8e–f), the effect of LiCl was compared to that of cAMP removal (−cAMP), as we have shown previously that withdrawal of cAMP analogs is sufficient to re-establish high levels of expression of immature markers such as c-Jun, GFAP and $p75^{NGFR}$ [31]. Data derived from these experiments suggested that LiCl effectively counteracted the effect of CPT-cAMP on maintaining high levels of expression of Krox-20 in mature, differentiated SCs and it did so in a specific manner (Fig. 8a–b). In the presence of cAMP, LiCl was not sufficient to re-establish the high levels of expression of c-Jun (Fig. 8e), $p75^{NGFR}$ (Fig. 8a) and GFAP (Fig. 8f) that are typical of immature (cycling) SCs. Albeit LiCl administration affected the cAMP-dependent maintenance of O1 and Prx expression, the magnitude of the inhibitory effect was much less pronounced than that seen for Krox-20 (Fig. 8a–f).

Overall, these results suggest that the lithium-dependent blockage of Krox-20 expression occurs without a concurrent increase in the expression of c-Jun or other immature SC markers. Though it seems clear that Krox-20 is a primary target of lithium's antagonistic action on cAMP-driven SC differentiation, lithium itself is insufficient to drive a reversal of the differentiated state in cAMP-treated SCs.

Lithium effectively prevents myelin formation without inducing myelin loss

The induction of myelin gene expression and consequent formation of myelin sheaths by SCs *in vitro* is dependent on the presence of L-ascorbic acid (vitamin C), [34]. It has been widely shown that provision of L-ascorbic acid to SC-DRG neuron cultures enables effective ensheathment of axons by SC processes, ECM deposition, basal lamina formation and myelin membrane wrapping [34]. These changes occur without the need to provide cAMP-stimulating agents. Given the physiological relevance of SC-DRG neuron cultures for the study of myelination, we next used immunofluorescence microscopy analysis to examine whether LiCl would prevent SC differentiation in ascorbate-treated SC-neuron cultures. For these experiments, purified SCs were seeded onto purified embryonic DRG neurons to allow re-population of the axonal outgrowth prior to providing ascorbic acid-supplemented medium in the absence or presence of LiCl. One week after the onset of ascorbate treatment, cultures were analyzed for the expression of the myelinating SC-specific markers O1 and myelin basic protein (MBP), as simultaneous detection of O1 and MBP serves to clearly discriminate myelin-forming (O1 positive/MBP positive) from non-myelin-forming (O1 negative, MBP negative) SCs within the co-culture system [30]. For reference purposes, these cultures were routinely stained with antibodies against NF, which revealed the extension of the axonal outgrowth, and DAPI, which revealed the relative density and distribution of SCs and neurons. Some cultures were also immunostained with antibodies recognizing cell surface O4, which was used to identify all axon-related SCs, and collagen type IV, a main constituent of the ECM used to indicate basal lamina assembly by axon-contacting SCs [34]. As evidenced by the panoramic and higher resolution immunofluorescence microscopy images presented in Figs. 9a and 9b, respectively, O1 and MBP expression was markedly reduced in LiCl-treated cultures, even when provided at low concentrations (7 mM). As expected, no myelin formation was observed in cultures maintained from the outset in the absence of ascorbate either when provided alone (Fig. 9a, control) or in the presence of LiCl (not shown). As shown by the quantitative data analysis

depicted in Fig. 9c, higher concentrations of LiCl (15–30 mM) abolished O1 and MBP expression in ascorbate-treated cultures (Fig. 9c), closely resembling the action of high doses of soluble Neu peptide (50 nM), which was used here as a positive control based on its well-known potent inhibitory activity on myelination in ascorbate-treated SC-neuron cultures (Fig. 9a), [36]. The widespread distribution of SCs expressing high levels of O4 in LiCl-treated cultures indicated that lithium prevented myelination without impoverishing the health of the SCs and neurons or their ability to interact with one another (Fig. 10a–b). In SC-neuron cultures, O4 expression only occurs in axon-related SCs (Fig. 10b) and its appearance on the SC surface is suggestive of a functional and stable physical association between SC processes and axons [42]. Likewise, the continued presence of LiCl did not interfere with the ascorbate-induced expression of collagen type IV (Fig. 10a–b). This result suggests that the impairment in myelin formation does not result from a deficiency in the SC's ability to deposit ECM in response to axon-derived signals [34]. No indication of impaired SC-axon alignment in LiCl-treated SC-neuron cultures was observed, either in the absence or presence of ascorbate (Fig. 10b and data not shown).

Given that soluble Neu can simultaneously induce myelin fragmentation in vitro [36], we next tested whether LiCl could have an adverse effect on fully-formed myelinating SCs. For these experiments, we simply delayed the administration of LiCl (or Neu as a control) with respect to the provision of L-ascorbic acid. In Fig. 11, a quantitative assessment of the overall optic density representing the intensity of O1, MBP and NF expression throughout the culture area is provided (Fig. 11a–d) along with an estimation of the density (Fig. 11e), length (Fig. 11g) and thickness (Fig. 11f) of individual myelinated fibers in local areas. Results from immunofluorescence microscopy analysis confirmed that soluble Neu rather than high doses of LiCl (15–30 mM) induced myelin degradation *in vitro*. Myelinating SCs in Neu-treated cultures exhibited shorter (Fig. 11h), heavily fragmented MBP positive segments along with extensively branched, O1 positive membrane processes (Fig. 11a). A moderate enhancement in the IOD of O1 and MBP expression was apparent in LiCl-treated cultures (Fig. 11a–c) possibly due to the mild increase detected in the length of individual myelin sheaths (Fig. 11g). Our analysis did not render significant differences in the density (Fig. 11e) or thickness of MBP positive fibers (Fig. 11f). Image data analysis of cultures stained with NF antibodies showed no evidence of axonal loss in response to LiCl or Neu treatment under the conditions of our experiments (Fig. 11a, lower panels, and d). Myelin fragmentation or loss of a compacted shape, which are two independent signs indicative of SC dedifferentiation, were not observed in LiCl-treated cultures.

Our combined data derived from isolated and axon-related SCs indicated that lithium blocks myelination by halting the onset of differentiation while preserving the integrity of pre-existing myelin sheaths.

Discussion

This study was initiated to investigate whether lithium could replace or enhance the effect of growth factors that use downstream effectors of the PI3-K signaling network to drive proliferation and/or differentiation into myelin-forming cells. Contrary to our expectations, we found that lithium not only failed to promote proliferation and differentiation of cultured

SCs but also prevented S-phase entry and the expression of myelin-specific markers when administered in conjunction with inductive signals such as Neu and cAMP, respectively. The antagonistic action of lithium on cell cycle progression and differentiation was sensitive to the presence/absence of lithium salts as inhibition was readily and specifically relieved upon lithium removal. Lithium had the unique ability to prevent differentiation and maintain high levels of expression of immature SC markers by overriding the pro-differentiating action of cAMP. It also prevented myelin formation without affecting the SC's ability to interact with axons or synthesize ECM components and it did so without inducing myelin degradation or SC dedifferentiation in mature, myelinating cells. The latter feature not only highlights lithium's safety but also distinguishes its mode of action from that of other extracellular signals (e.g. soluble Neu) and intracellular transcription factors (e.g. c-Jun) that are known to have a dual action in blocking myelination and inducing myelin loss [18,36].

Understanding the molecular mechanism by which lithium exerts biological effects in SCs requires further investigation. Dose response studies highlighted the need of concentrations of LiCl in the millimolar range in order to observe inhibition of SC proliferation, differentiation and GSK-3β activity. Of note, this range of concentration is consistent with previous *in vitro* studies in SCs ([22] - 10 mM; [25] - 16 mM) and oligodendrocytes ([43], 20–30 mM). Importantly, the administration of relatively high doses of LiCl did not hinder specificity of action, as LiCl-dependent changes in SC morphology, proliferation and differentiation could not be mimicked by equimolar doses of NaCl or KCl. We interpreted this data as an indication of the high specificity of action of LiCl versus that of other chloride salts that are completely ionized in water and provide the same osmolarity in solution. Lithium is the closest physiological analog to sodium and enters to the cell primarily via sodium transporters following a concentration gradient and without energy consumption. Given that these transporters, mainly Na^+/H^+ exchangers and Na^+-dependent co-transporting systems, bind sodium and lithium with similar affinities, the membrane permeability to these ions has been shown to be similar [44–46]. Thus, we cannot explain the action of LiCl simply on the basis of hyperosmolar or depolarizing effects and suggest that lithium-specific intracellular mechanisms and effectors are required.

How lithium mediates its pharmacological effects is still a matter of controversy. Yet, at the molecular level, it is well-recognized that lithium acts primarily as an inhibitor of the activity of GSK-3β through direct and indirect mechanisms. On one hand, lithium can directly inhibit the activity of GSK-3β by competing with the co-factor Mg^{+2} for direct binding to the kinase [47]. On the other hand, lithium inhibits GSK-3β activity by enhancing the phosphorylation on Ser-9, an inhibitory site for GSK-3β, through increasing the activity of upstream kinase Akt [48,49] or decreasing the activity of Ser-9-specific phosphatases [1,50]. In turn, by means of downregulation of GSK-3β activity, lithium affects multiple signaling systems including Wnt/β-catenin [51,52] which is implicated in the differentiation of glial cells and myelinogenesis both in the peripheral and central nervous systems [26,53]. Though lithium mimicked the effect of Neu/ErbB activity on GSK-3β inactivation and β-catenin accumulation, as expected, lithium failed to mimic Neu's effect on SC proliferation [33]. As opposed to Neu, lithium specifically, dose-dependently and reversibly arrested cells in the cell cycle and inhibited S-phase progression without affecting cell survival. One important aspect of the lithium-dependent proliferation blockage was the reversibility of the

effect, as SCs could readily re-enter the S-phase right after the removal of lithium compounds. Intriguingly, an early study suggested that lithium increases the mitogenic activity of axolemma- and myelin-enriched fractions in cultured postnatal SCs [24]. Even though the basis for the discrepancy with our results is unclear, accumulated research has shown that the outcome in cell proliferation can be cell type-, context- and stimulus-dependent. An anti-mitogenic action of lithium has been reported primarily in cancer cells from colon, neuroblastoma and leukemia [54–56]. In normal cells, on the contrary, both the action of lithium and that of GSK-3β inhibitors has been prevalently linked to an increase rather than a decrease in cell proliferation rates. Examples are neural precursor and mesenchymal stem cells that respond to lithium treatment by undergoing proliferation, typically in a GSK-3β/β-catenin-dependent manner [2,3]. Whether lithium compounds differentially affect the proliferation of normal and cancer SCs remains an open but intriguing question.

In addition to inducing cell cycle arrest, prolonged lithium treatment also promoted substantial cell flattening, enlargement and vacuolization of the cytoplasm, somehow resembling the pro-differentiating action of cAMP in cultured isolated SCs. Besides, lithium suppressed the expression of c-Jun/AP1, an event that has been associated with a halt in proliferation and onset of myelination [38]. Nevertheless, and as opposed to cAMP, we observed that these changes occurred without a concomitant increase in the expression of myelination-associated markers. Lithium-induced changes were highly reversible, as lithium withdrawal was sufficient to restore the proliferative potential and the bipolar shape typical of immature, cycling cells. Not only did lithium exert a strong antagonistic action on the cAMP-dependent expression of various myelin-related proteins and lipids but also virtually abrogated myelin sheath formation *in vitro*. Curiously, lithium-treated SCs were able to maintain high levels of expression of various markers indicative of an immature state even in the presence of cAMP and low levels of c-Jun. The blockage of c-Jun expression by lithium has been documented previously [57,58] and may explain the antagonistic action on SC proliferation [59]. However, our studies differ from existing literature reporting induction of myelin gene expression in response to lithium in SCs [25,22] and oligodendrocytes [60,43]. The study by Ogata et al [25] reported that co-stimulation of postnatal rat SCs with LiCl (16 mM) and Fsk increased the levels of MAG mRNA. The study by Makoukji [22] reported that LiCl (10 mM) increased the mRNA of P_0 and PMP22 24 h post-stimulation in a SC line (MSC80) and primary postnatal mouse SCs. An increase in myelin thickness and acceleration of functional recovery after crush injuries of the facial and sciatic nerves in mice were also reported [22]. The basis for the apparent discrepancy with our results is likely due to aspects such as diverse as the model systems used, the potency and duration of treatment, the outcome measures and/or context-specific variation in signaling outcome. Whether the SC's responses to lithium would change as a function of the stimulus (e.g. Neu versus axonal membranes), the stage of differentiation of the cells (eg. adult versus postnatal cells) or the species (rat versus mice) is not known. For instance, we have shown that the time of lithium administration with respect to the administration of the stimulus critically alters the outcome of Neu- and cAMP-dependent proliferation and myelin marker expression, respectively. Inhibition of cell differentiation in response to lithium rarely occurs but this has been reported in osteogenic cell lines [61]. A recent study which used lithium to

increase autophagy in dissociated SCs and cultured nerve segments undergoing Wallerian degeneration provided evidence on a novel use of lithium to enhance myelin engulfment and accelerate the rate of myelin protein breakdown [62]. Though we have not seen evidence indicating that lithium could induce autophagy and/or myelin degradation in intact myelinating SC-neuron cultures, it is possible that the extensive vacuolization of the cytoplasm we have observed in isolated lithium-treated SCs results from an increased autophagic activity. So far, whether lithium aids in myelin clearance during Wallerian degeneration *in vitro* or *in vivo* has not been addressed in previous studies and remains an attractive direction for future research.

The blockage of SC differentiation by lithium most likely relies on inhibition of Krox-20. Nevertheless, how lithium inhibits cAMP-driven Krox-20 expression is still uncertain. Though it is possible that this is dependent on the inhibition of GSK-3β, research has shown that not all signals reducing GSK-3β activity would antagonize Krox-20 expression. For instance, Neu and other growth factors such as insulin-like growth factor and fibroblast growth factor effectively activate Akt and inhibit GSK-3β activity in SCs but none of these factors antagonize the cAMP-driven expression of Krox-20 or that of other myelin-associated genes [63,64]. In addition to targeting GSK-3β, lithium inhibits the activity of several adenylyl cyclase isoforms [65] and modulates the levels of various intermediaries within the phosphatidylinositol (PI) pathway [66]. It is well-established that therapeutically relevant doses of lithium block the activity of inositol monophosphatase (IMPase) and inositol polyphosphatase-1 (IPP1), which are two key enzymes involved in phosphatidylinositol 4,5-bisphosphate (PIP_2) recycling. Inhibition of IMPase and IPP1 by lithium leads to depletion of inositide reserves, which in turn indirectly interferes with the biosynthesis of the second messengers inositol trisphosphate and diacylglycerol in response to extracellular signals that activate phospholipase C (PLC) [67]. Interestingly, PLC is a key downstream effector of both tyrosine kinase and G protein-coupled receptors. Whether impaired inositide recycling or PLC activity contribute to lithium's inhibition of ErbB- and/or cAMP-dependent signaling in SCs is not known. Though current research supports the notion that GSK-3β and enzymes of PI metabolism are strong candidates to mediate lithium's effects in mammalian cells in general, further experiments are required in order to elucidate their particular role, if any, in lithium's inhibitory action on SC proliferation and/or myelination. Interestingly, it has been shown previously that that induction of autophagy by lithium relies on impaired inositol recycling [68].

It is currently understood that the initiation and maintenance of a myelinated state depends on the balance between positive and negative transcriptional regulators of myelination [41]. However, further research is needed to identify the broad spectrum of extracellular signals and intracellular pathways involved in this regulation. Negative regulators of myelination are expected to prevent myelination, counterbalance the action of pro-differentiating signals and actively aid in the SC's conversion into repair cells through inducing their dedifferentiation (reprogramming) and ability to break down myelin, an event recently referred to as myelinophagy [62]. The most widely understood negative regulator of myelination is c-Jun, a transcriptional inhibitor of myelination and promoter of the repair phenotype after nerve injury [69]. To the best of our knowledge, lithium is the first described reversible antagonist of SC differentiation that blocks the onset of myelination without inducing myelin loss, SC

dedifferentiation or c-Jun expression. Given its ability to preclude the SC's transition into a Krox-20 positive state independently of c-Jun upregulation, lithium provides us with a unique way to pharmacologically interfere with the onset of myelination. In addition, the reversibility of lithium's action on cAMP-induced SC differentiation and Krox-20 expression is ideal to delay and possibly synchronize the onset of myelination by endogenous or exogenous (transplanted) SCs, and thereby maximize the efficiency of nerve tissue repair and re-myelination [70]. The newly discovered potential of lithium to increase myelin clearance via direct induction of myelinophagy can represent a still-to-be explored beneficial feature for the use of lithium therapy to foster peripheral nerve regeneration.

Our results from *in vitro* assays underscored a previously unforeseen role of lithium as dual reversible inhibitor of SC proliferation and differentiation. To validate our data, we combined the use of independent model systems consisting of isolated SCs and SC-DRG neuron cultures due to the advantage they provide in terms of simplicity and physiological relevance, respectively. Experiments using SC-only cultures are easy to set up, and allow multiple experimental variables and readouts to be tested in parallel samples, thereby facilitating interpretation of mechanistic results. Throughout these studies, we used Neu and cAMP as inductive signals for proliferation and differentiation, respectively, to maximize the cellular responses in cell division and myelin gene expression in the absence of neurons [31,35]. Results from differentiation assays were confirmed using SC-neuron cultures prepared under standard conditions supportive of myelination. Despite these cultures are labor-intensive and time-consuming to prepare, they have no parallel to address questions on SC-axon interactions and myelination that could not be addressed otherwise. In addition, we have run numerous controls for lithium's activity, specificity, dose dependency, and pathway activation and studied the reversibility of lithium's action on proliferation and differentiation for the first time. So far, it is uncertain how much our results from *in vitro* assays could be relevant *in vivo.* In particular, whether lithium reversibly affects the outcome of SC proliferation, Krox-20 expression and myelination in organotypic cultures and peripheral nerves throughout development, with and without injury, requires more extensive investigation. Because the doses of lithium herein used cannot be used in clinical therapy, we anticipate the need for further research in order to better assess the potential for translation.

A series of studies have documented favorable effects of lithium in the peripheral nervous system. Two independent studies have concluded that lithium promotes earlier motor functional recovery by initially accelerating the growth rate of regenerated axons and enhancing remyelination [71,22]. Results from Nouri et al. suggest that lithium improves sciatic nerve regeneration after a traumatic lesion [72]. Additional evidence indicates that lithium exhibits synergistic effects in combined therapies with glial-derived neurotrophic factor in a model of rat sciatic nerve injury [23] and enhances the regenerative capacity of spinal motorneurons in a rat model of brachial plexus root avulsion [73]. To conclude, lithium's pharmacology and biological effects in human patients have been extensively documented and its benefits on the central and peripheral nervous systems are seemingly clear. By means of its reversible mode of action, lithium provides us with a novel candidate pharmacological tool to safely control the extent and rate of expansion and myelin formation by SCs in a variety of experimental paradigms.

Supplementary Material

Refer to Web version on PubMed Central for supplementary material.

Acknowledgments

We thank the excellent technical support provided by Jennifer Soto and Ketty Bacallao with neuronal cell cultures. We kindly acknowledge the assistance provided by Vladimir Camarena and Gaofeng Wang with IncuCyte microscopy, Melissa Carballosa with ImageJ software and Yan Shi with automated fluorescence microscopy. This work was supported by NIH-NINDS (NS084326), The Craig H. Neilsen Foundation, The Miami Project to Cure Paralysis and The Buoniconti Fund. G.P. was a recipient of a CONICET/BecAr fellowship (Argentina).

References

1. Jope R. Lithium and GSK-3: one inhibitor, two inhibitory actions, multiple outcomes. Trends Pharmacol Sci. 2003; 24(9):441–443. [PubMed: 12967765]
2. Kim JS, Chang MY, Yu IT, Kim JH, Lee SH, Lee YS, Son H. Lithium selectively increases neuronal differentiation of hippocampal neural progenitor cells both in vitro and in vivo. J Neurochem. 2004; 89(2):324–336. [PubMed: 15056276]
3. Zhu Z, Yin J, Guan J, Hu B, Niu X, Jin D, Wang Y, Zhang C. Lithium stimulates human bone marrow derived mesenchymal stem cell proliferation through GSK-3beta-dependent beta-catenin/Wnt pathway activation. FEBS J. 2014; 281(23):5371–5389. [PubMed: 25265417]
4. Su H, Chu TH, Wu W. Lithium enhances proliferation and neuronal differentiation of neural progenitor cells in vitro and after transplantation into the adult rat spinal cord. Exp Neurol. 2007; 206(2):296–307. [PubMed: 17599835]
5. Arioka M, Takahashi-Yanaga F, Sasaki M, Yoshihara T, Morimoto S, Hirata M, Mori Y, Sasaguri T. Acceleration of bone regeneration by local application of lithium: Wnt signal-mediated osteoblastogenesis and Wnt signal-independent suppression of osteoclastogenesis. Biochem Pharmacol. 2014; 90(4):397–405. [PubMed: 24955980]
6. Salzer JL. Schwann cell myelination. Cold Spring Harb Perspect Biol. 2015; 7(8):a020529. [PubMed: 26054742]
7. Jessen KR, Mirsky R. The origin and development of glial cells in peripheral nerves. Nat Rev Neurosci. 2005; 6(9):671–682. [PubMed: 16136171]
8. Morrissey TK, Levi AD, Nuijens A, Sliwkowski MX, Bunge RP. Axon-induced mitogenesis of human Schwann cells involves heregulin and p185erbB2. Proc Natl Acad Sci U S A. 1995; 92(5): 1431–1435. [PubMed: 7877996]
9. Birchmeier C, Nave KA. Neuregulin-1, a key axonal signal that drives Schwann cell growth and differentiation. Glia. 2008; 56(14):1491–1497. [PubMed: 18803318]
10. Maurel P, Salzer JL. Axonal regulation of Schwann cell proliferation and survival and the initial events of myelination requires PI 3-kinase activity. The Journal of neuroscience : the official journal of the Society for Neuroscience. 2000; 20(12):4635–4645. [PubMed: 10844033]
11. Chen P, Cescon M, Bonaldo P. The Role of Collagens in Peripheral Nerve Myelination and Function. Mol Neurobiol. 2015; 52(1):216–225. [PubMed: 25143238]
12. Heller BA, Ghidinelli M, Voelkl J, Einheber S, Smith R, Grund E, Morahan G, Chandler D, Kalaydjieva L, Giancotti F, King RH, Fejes-Toth AN, Fejes-Toth G, Feltri ML, Lang F, Salzer JL. Functionally distinct PI 3-kinase pathways regulate myelination in the peripheral nervous system. The Journal of cell biology. 2014; 204(7):1219–1236. [PubMed: 24687281]
13. Bschor T. Lithium in the treatment of major depressive disorder. Drugs. 2014; 74(8):855–862. [PubMed: 24825489]
14. Li H, Li Q, Du X, Sun Y, Wang X, Kroemer G, Blomgren K, Zhu C. Lithium-mediated long-term neuroprotection in neonatal rat hypoxia-ischemia is associated with antiinflammatory effects and enhanced proliferation and survival of neural stem/progenitor cells. J Cereb Blood Flow Metab. 2011; 31(10):2106–2115. [PubMed: 21587270]

15. Cabrera O, Dougherty J, Singh S, Swiney BS, Farber NB, Noguchi KK. Lithium protects against glucocorticoid induced neural progenitor cell apoptosis in the developing cerebellum. Brain Res. 2014; 1545:54–63. [PubMed: 24361977]

16. De Sarno P, Axtell RC, Raman C, Roth KA, Alessi DR, Jope RS. Li prevents and ameliorates experimental autoinmune encephalomyelitis. J Immunol. 2008; 181(1):338–345. [PubMed: 18566399]

17. Huo K, Sun Y, Li H, Du X, Wang X, Karlsson N, Zhu C, Blomgren K. Lithium reduced neural progenitor apoptosis in the hippocampus and ameliorated functional deficits after irradiation to the immature mouse brain. Mol Cell Neurosci. 2012; 51(1–2):32–42. [PubMed: 22800605]

18. Yang ML, Li JJ, So KF, Chen JY, Cheng WS, Wu J, Wang ZM, Gao F, Young W. Efficacy and safety of lithium carbonate treatment of chronic spinal cord injuries: a double-blind, randomized, placebo-controlled clinical trial. Spinal Cord. 2012; 50(2):141–146. [PubMed: 22105463]

19. Dill J, Wang H, Zhou F, Li S. Inactivation of glycogen synthase kinase 3 promotes axonal growth and recovery in the CNS. The Journal of neuroscience : the official journal of the Society for Neuroscience. 2008; 28(36):8914–8928. [PubMed: 18768685]

20. Lazzara CA, Kim YH. Potential application of lithium in Parkinson's and other neurodegenerative diseases. Front Neurosci. 2015; 9:403. [PubMed: 26578864]

21. Diniz BS, Machado-Vieira R, Forlenza OV. Lithium and neuroprotection: translational evidence and implications for the treatment of neuropsychiatric disorders. Neuropsychiatr Dis Treat. 2013; 9:493–500. [PubMed: 23596350]

22. Makoukji J, Belle M, Meffre D, Stassart R, Grenier J, Shackleford G, Fledrich R, Fonte C, Branchu J, Goulard M, de Waele C, Charbonnier F, Sereda MW, Baulieu EE, Schumacher M, Bernard S, Massaad C. Lithium enhances remyelination of peripheral nerves. Proc Natl Acad Sci U S A. 2012; 109(10):3973–3978. [PubMed: 22355115]

23. Lin YC, Oh SJ, Marra KG. Synergistic lithium chloride and glial cell line-derived neurotrophic factor delivery for peripheral nerve repair in a rodent sciatic nerve injury model. Plastic and reconstructive surgery. 2013; 132(2):251e–262e. [PubMed: 23897324]

24. Yoshino JE, DeVries GH. Effect of lithium on Schwann cell proliferation stimulated by axolemma- and myelin-enriched fractions. J Neurochem. 1987; 48(4):1270–1277. [PubMed: 3819729]

25. Ogata T, Iijima S, Hoshikawa S, Miura T, Yamamoto S, Oda H, Nakamura K, Tanaka S. Opposing extracellular signal-regulated kinase and Akt pathways control Schwann cell myelination. The Journal of neuroscience : the official journal of the Society for Neuroscience. 2004; 24(30):6724–6732. [PubMed: 15282275]

26. Meffre D, Grenier J, Bernard S, Courtin F, Dudev T, Shackleford G, Jafarian-Tehrani M, Massaad C. Wnt and lithium: a common destiny in the therapy of nervous system pathologies? Cell Mol Life Sci. 2014; 71(7):1123–1148. [PubMed: 23749084]

27. Morrissey TK, Kleitman N, Bunge RP. Isolation and functional characterization of Schwann cells derived from adult peripheral nerve. The Journal of neuroscience : the official journal of the Society for Neuroscience. 1991; 11(8):2433–2442. [PubMed: 1869923]

28. Brockes JP, Fields KL, Raff MC. Studies on cultured rat Schwann cellsIEstablishment of purified populations from cultures of peripheral nerve. Brain Res. 1979; 165(1):105–118. [PubMed: 371755]

29. Monje PV, Rendon S, Athauda G, Bates M, Wood PM, Bunge MB. Non-antagonistic relationship between mitogenic factors and cAMP in adult Schwann cell re-differentiation. Glia. 2009; 57(9): 947–961. [PubMed: 19053056]

30. Bacallao K, Monje PV. Requirement of cAMP signaling for Schwann cell differentiation restricts the onset of myelination. PLoS One. 2015; 10(2):e0116948. [PubMed: 25705874]

31. Monje PV, Soto J, Bacallao K, Wood PM. Schwann cell dedifferentiation is independent of mitogenic signaling and uncoupled to proliferation: role of cAMP and JNK in the maintenance of the differentiated state. J Biol Chem. 2010; 285(40):31024–31036. [PubMed: 20634285]

32. Riss, TL., Moravec, RA., Niles, AL., Benink, HA., Worzella, TJ., Minor, L. Cell Viability Assays. In: Sittampalam, GS.Coussens, NP.Nelson, H., et al., editors. Assay Guidance Manual. Bethesda (MD): Eli Lilly & Company and the National Center for Advancing Translational Sciences; 2004.

33. Monje PV, Bartlett Bunge M, Wood PM. Cyclic AMP synergistically enhances neuregulin-dependent ERK and Akt activation and cell cycle progression in Schwann cells. Glia. 2006; 53(6): 649–659. [PubMed: 16470843]
34. Eldridge CF, Bunge MB, Bunge RP, Wood PM. Differentiation of axon-related Schwann cells in vitroIAscorbic acid regulates basal lamina assembly and myelin formation. The Journal of cell biology. 1987; 105(2):1023–1034. [PubMed: 3624305]
35. Bacallao K, Monje PV. Opposing roles of PKA and EPAC in the cAMP-dependent regulation of schwann cell proliferation and differentiation [corrected]. PLoS One. 2013; 8(12):e82354. [PubMed: 24349260]
36. Syed N, Reddy K, Yang DP, Taveggia C, Salzer JL, Maurel P, Kim HA. Soluble neuregulin-1 has bifunctional, concentration-dependent effects on Schwann cell myelination. The Journal of neuroscience : the official journal of the Society for Neuroscience. 2010; 30(17):6122–6131. [PubMed: 20427670]
37. Sobue G, Shuman S, Pleasure D. Schwann cell responses to cyclic AMP: proliferation, change in shape, and appearance of surface galactocerebroside. Brain Res. 1986; 362(1):23–32. [PubMed: 3002553]
38. Parkinson DB, Bhaskaran A, Arthur-Farraj P, Noon LA, Woodhoo A, Lloyd AC, Feltri ML, Wrabetz L, Behrens A, Mirsky R, Jessen KR. c-Jun is a negative regulator of myelination. The Journal of cell biology. 2008; 181(4):625–637. [PubMed: 18490512]
39. Morgan L, Jessen KR, Mirsky R. The effects of cAMP on differentiation of cultured Schwann cells: progression from an early phenotype (04+) to a myelin phenotype (P0+, GFAP−, N-CAM−, NGF-receptor-) depends on growth inhibition. The Journal of cell biology. 1991; 112(3):457–467. [PubMed: 1704008]
40. Jessen KR, Mirsky R. Negative regulation of myelination: relevance for development, injury, and demyelinating disease. Glia. 2008; 56(14):1552–1565. [PubMed: 18803323]
41. Jessen KR, Mirsky R. The repair Schwann cell and its function in regenerating nerves. J Physiol. 2016; 594(13):3521–3531. [PubMed: 26864683]
42. Mirsky R, Dubois C, Morgan L, Jessen KR. 04 and A007-sulfatide antibodies bind to embryonic Schwann cells prior to the appearance of galactocerebroside; regulation of the antigen by axon-Schwann cell signals and cyclic AMP. Development (Cambridge, England). 1990; 109(1):105–116.
43. Azim K, Butt AM. GSK3beta negatively regulates oligodendrocyte differentiation and myelination in vivo. Glia. 2011; 59(4):540–553. [PubMed: 21319221]
44. Holstein-Rathlou NH. Lithium transport across biological membranes. Kidney international Supplement. 1990; 28:S4–S9. [PubMed: 2182930]
45. Timmer RT, Sands JM. Lithium intoxication. Journal of the American Society of Nephrology : JASN. 1999; 10(3):666–674. [PubMed: 10073618]
46. Iurinskaia VE, Moshkov AV, Goriachaia TS, Vereninov AA. [Li/Na exchange and Li active transport in human lymphoid cells U937 cultured in lithium media]. Tsitologiia. 2013; 55(10): 703–712. [PubMed: 25509124]
47. Dudev T, Lim C. Competition between Li+ and Mg2+ in metalloproteins. Implications for lithium therapy. J Am Chem Soc. 2011; 133(24):9506–9515. [PubMed: 21595457]
48. Pan JQ, Lewis MC, Ketterman JK, Clore EL, Riley M, Richards KR, Berry-Scott E, Liu X, Wagner FF, Holson EB, Neve RL, Biechele TL, Moon RT, Scolnick EM, Petryshen TL, Haggarty SJ. AKT kinase activity is required for lithium to modulate mood-related behaviors in mice. Neuropsychopharmacology. 2011; 36(7):1397–1411. [PubMed: 21389981]
49. Beaulieu JM, Marion S, Rodriguiz RM, Medvedev IO, Sotnikova TD, Ghisi V, Wetsel WC, Lefkowitz RJ, Gainetdinov RR, Caron MG. A beta-arrestin 2 signaling complex mediates lithium action on behavior. Cell. 2008; 132(1):125–136. [PubMed: 18191226]
50. Beurel E, Grieco SF, Jope RS. Glycogen synthase kinase-3 (GSK3): regulation, actions, and diseases. Pharmacol Ther. 2015; 148:114–131. [PubMed: 25435019]
51. Hoppler S, Kavanagh C. Wnt signalling: variety at the core. Journal of Cell Science. 2006; 120:385–393.

52. Lien WH, Fuchs E. Wnt some lose some: transcriptional governance of stem cells by Wnt/beta-catenin signaling. Genes Dev. 2014; 28(14):1517–1532. [PubMed: 25030692]
53. Tawk M, Makoukji J, Belle M, Fonte C, Trousson A, Hawkins T, Li H, Ghandour S, Schumacher M, Massaad C. Wnt/beta-catenin signaling is an essential and direct driver of myelin gene expression and myelinogenesis. The Journal of neuroscience : the official journal of the Society for Neuroscience. 2011; 31(10):3729–3742. [PubMed: 21389228]
54. Pizarro JG, Folch J, Esparza JL, Jordan J, Pallas M, Camins A. A molecular study of pathways involved in the inhibition of cell proliferation in neuroblastoma B65 cells by the GSK-3 inhibitors lithium and SB-415286. J Cell Mol Med. 2009; 13(9B):3906–3917. [PubMed: 18624766]
55. Trnski D, Sabol M, Gojevic A, Martinic M, Ozretic P, Musani V, Ramic S, Levanat S. GSK3beta and Gli3 play a role in activation of Hedgehog-Gli pathway in human colon cancer - Targeting GSK3beta downregulates the signaling pathway and reduces cell proliferation. Biochim Biophys Acta. 2015; 1852(12):2574–2584. [PubMed: 26385428]
56. Zassadowski F, Pokorna K, Ferre N, Guidez F, Llopis L, Chourbagi O, Chopin M, Poupon J, Fenaux P, Ann Padua R, Pla M, Chomienne C, Cassinat B. Lithium chloride antileukemic activity in acute promyelocytic leukemia is GSK-3 and MEK/ERK dependent. Leukemia. 2015; 29(12): 2277–2284. [PubMed: 26108692]
57. Hongisto V, Smeds N, Brecht S, Herdegen T, Courtney MJ, Coffey ET. Lithium Blocks the c-Jun Stress Response and Protects Neurons via Its Action on Glycogen Synthase Kinase 3. Molecular and Cellular Biology. 2003; 23(17):6027–6036. [PubMed: 12917327]
58. Jin N, Kovacs AD, Sui Z, Dewhurst S, Maggirwar SB. Opposite effects of lithium and valproic acid on trophic factor deprivation-induced glycogen synthase kinase-3 activation, c-Jun expression and neuronal cell death. Neuropharmacology. 2005; 48(4):576–583. [PubMed: 15755485]
59. Parkinson DB, Bhaskaran A, Droggiti A, Dickinson S, D'Antonio M, Mirsky R, Jessen KR. Krox-20 inhibits Jun-NH2-terminal kinase/c-Jun to control Schwann cell proliferation and death. The Journal of cell biology. 2004; 164(3):385–394. [PubMed: 14757751]
60. Meffre D, Massaad C, Grenier J. Lithium chloride stimulates PLP and MBP expression in oligodendrocytes via Wnt/beta-catenin and Akt/CREB pathways. Neuroscience. 2015; 284:962–971. [PubMed: 25451297]
61. Li J, Khavandgar Z, Lin SH, Murshed M. Lithium chloride attenuates BMP-2 signaling and inhibits osteogenic differentiation through a novel WNT/GSK3- independent mechanism. Bone. 2011; 48(2):321–331. [PubMed: 20932949]
62. Gomez-Sanchez JA, Carty L, Iruarrizaga-Lejarreta M, Palomo-Irigoyen M, Varela-Rey M, Griffith M, Hantke J, Macias-Camara N, Azkargorta M, Aurrekoetxea I, De Juan VG, Jefferies HB, Aspichueta P, Elortza F, Aransay AM, Martinez-Chantar ML, Baas F, Mato JM, Mirsky R, Woodhoo A, Jessen KR. Schwann cell autophagy, myelinophagy, initiates myelin clearance from injured nerves. The Journal of cell biology. 2015; 210(1):153–168. [PubMed: 26150392]
63. Monje PV, Athauda G, Wood PM. Protein kinase A-mediated gating of neuregulin-dependent ErbB2-ErbB3 activation underlies the synergistic action of cAMP on Schwann cell proliferation. J Biol Chem. 2008; 283(49):34087–34100. [PubMed: 18799465]
64. Arthur-Farraj P, Wanek K, Hantke J, Davis CM, Jayakar A, Parkinson DB, Mirsky R, Jessen KR. Mouse schwann cells need both NRG1 and cyclic AMP to myelinate. Glia. 2011; 59(5):720–733. [PubMed: 21322058]
65. Mann L, Heldman E, Shaltiel G, Belmaker RH, Agam G. Lithium preferentially inhibits adenylyl cyclase V and VII isoforms. Int J Neuropsychopharmacol. 2008; 11(4):533–539. [PubMed: 18205980]
66. Berridge MD P, Hanley M. Neural and developmental actions of lithium. Cell. 1989; 59:411–419. [PubMed: 2553271]
67. Brown K, Tracy D. Lithium: the pharmacodynamic actions of the amazing ion. Therapeutic Advances in Psychopharmacology. 2013; 3(3):163–176. [PubMed: 24167688]
68. Sarkar S, Floto RA, Berger Z, Imarisio S, Cordenier A, Pasco M, Cook LJ, Rubinsztein DC. Lithium induces autophagy by inhibiting inositol monophosphatase. The Journal of cell biology. 2005; 170(7):1101–1111. [PubMed: 16186256]

69. Arthur-Farraj PJ, Latouche M, Wilton DK, Quintes S, Chabrol E, Banerjee A, Woodhoo A, Jenkins B, Rahman M, Turmaine M, Wicher GK, Mitter R, Greensmith L, Behrens A, Raivich G, Mirsky R, Jessen KR. c-Jun reprograms Schwann cells of injured nerves to generate a repair cell essential for regeneration. Neuron. 2012; 75(4):633–647. [PubMed: 22920255]

70. Monje PV. To myelinate or not to myelinate: fine tuning cAMP signaling in Schwann cells to balance cell proliferation and differentiation. Neural Regen Res. 2015; 10(12):1936–1937. [PubMed: 26889176]

71. Fang XY, Zhang WM, Zhang CF, Wong WM, Li W, Wu W, Lin JH. Lithium accelerates functional motor recovery by improving remyelination of regenerating axons following ventral root avulsion and reimplantation. Neuroscience. 2016; 329:213–225. [PubMed: 27185485]

72. Nouri M, Rasouli MR, Rahimian R, Asadi-Amoli F, Dehpour AR. Lithium improves regeneration after sciatic nerve traumatic injury in rat. Journal of reconstructive microsurgery. 2009; 25(2):151. [PubMed: 19037843]

73. Fu R, Tang Y, Ling ZM, Li YQ, Cheng X, Song FH, Zhou LH, Wu W. Lithium enhances survival and regrowth of spinal motoneurons after ventral root avulsion. BMC neuroscience. 2014; 15:84. [PubMed: 24985061]

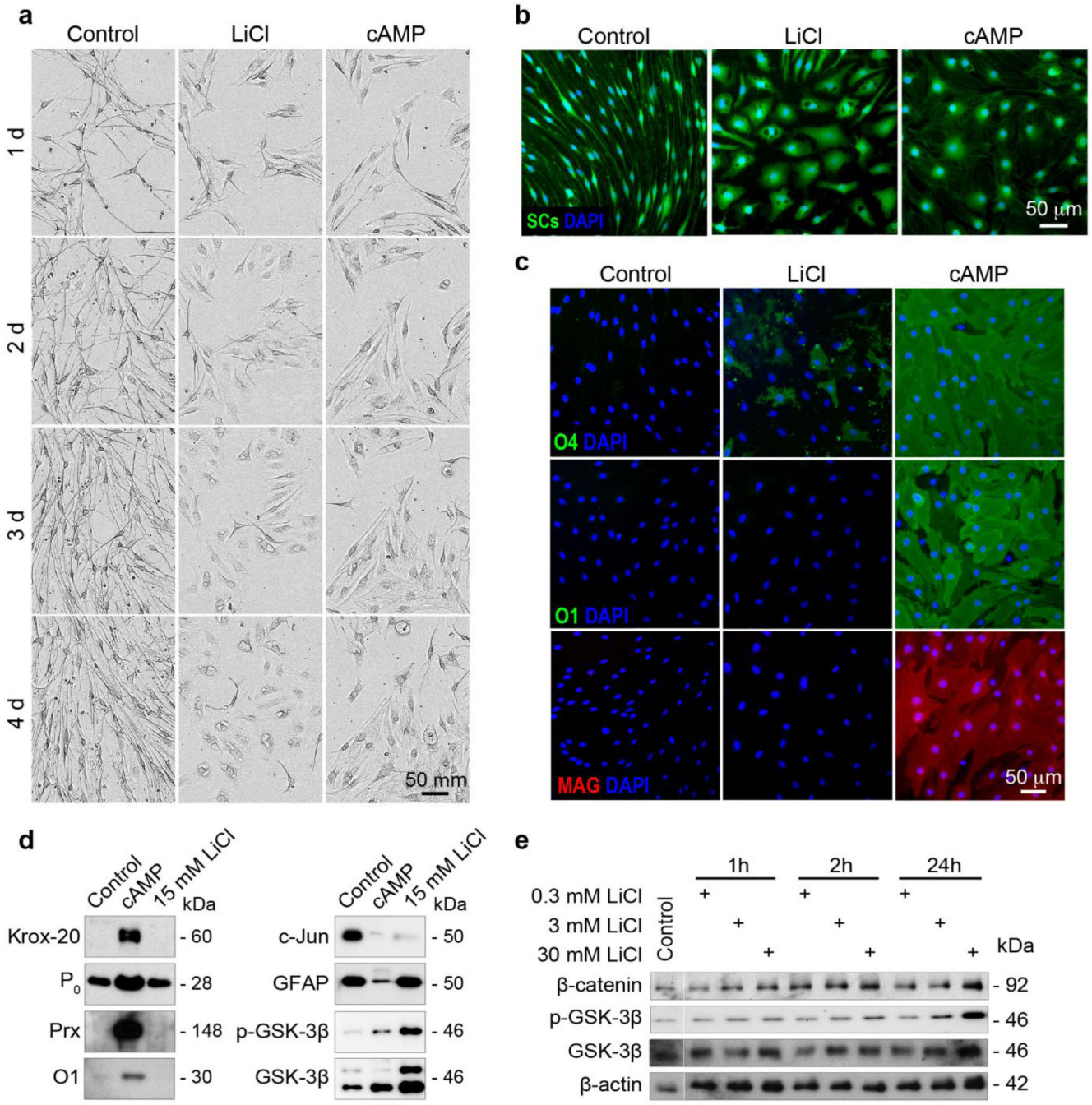

Fig. 1.

Prolonged stimulation with LiCl induces morphological changes in the absence of increased myelin marker expression in isolated primary SCs, **a** Time dependency of morphological changes induced by LiCl. IncuCyte ZOOM™ live cell imaging was used to register the temporal course of morphological changes induced by treatment with LiCl or cAMP (250 μM) in medium consisting of DMEM and 10% FBS (control). Phase contrast images were taken every 2 hours using 20X objective lenses. Selected areas and time points are shown to denote the most prominent morphological changes observed in individual cells throughout

time (d: days). Video imaging data of cAMP-treated cells taken at the same time points are provided for a side-by-side comparative analysis. Note the loss of contrast in LiCl- and cAMP-treated cultures undergoing progressive expansion and flattening of the cytoplasm. Cells treated with cAMP were used as a positive control for the induction of morphological changes and myelin marker expression. LiCl was used at 30 mM unless indicated. **b** Features of the morphological transformation induced by prolonged incubation with LiCl. SC cultures treated for 6 days with LiCl or cAMP were fluorescently labeled with CellTracker® Green, imaged by fluorescence microscopy and subsequently fixed for immunofluorescence microscopy analysis (**c**). Representative 20X magnification pictures are shown to denote the dramatic changes in cell shape and size that occur in response to LiCl and cAMP treatment, including the appearance of cytoplasmic vacuoles. Nuclei were counterstained with DAPI in all fluorescence microscopy images unless otherwise indicated. **c–d** Lack of changes in the expression of markers of differentiation in LiCl-treated SCs. Immunofluorescence microscopy (**c**) and western blot analysis (**d**) of the indicated SC-specific markers revealed no significant changes in the expression of myelinating SC markers. Panel **d** includes profiles of GSK-3β phosphorylation (Serine-9) and expression (total levels) to confirm the LiCl-dependent inactivation of GSK-3β. **e** Dose response and time course dependency of GSK-3β phosphorylation and β-catenin expression in LiCl-treated SCs. Cells were treated with increasing concentrations of LiCl (as indicated) and collected for western blot analysis at 1, 2 and 24 h post-stimulation. Increased β-catenin levels are likely due to reduced degradation of the β-catenin protein in response to GSK-3β inactivation.

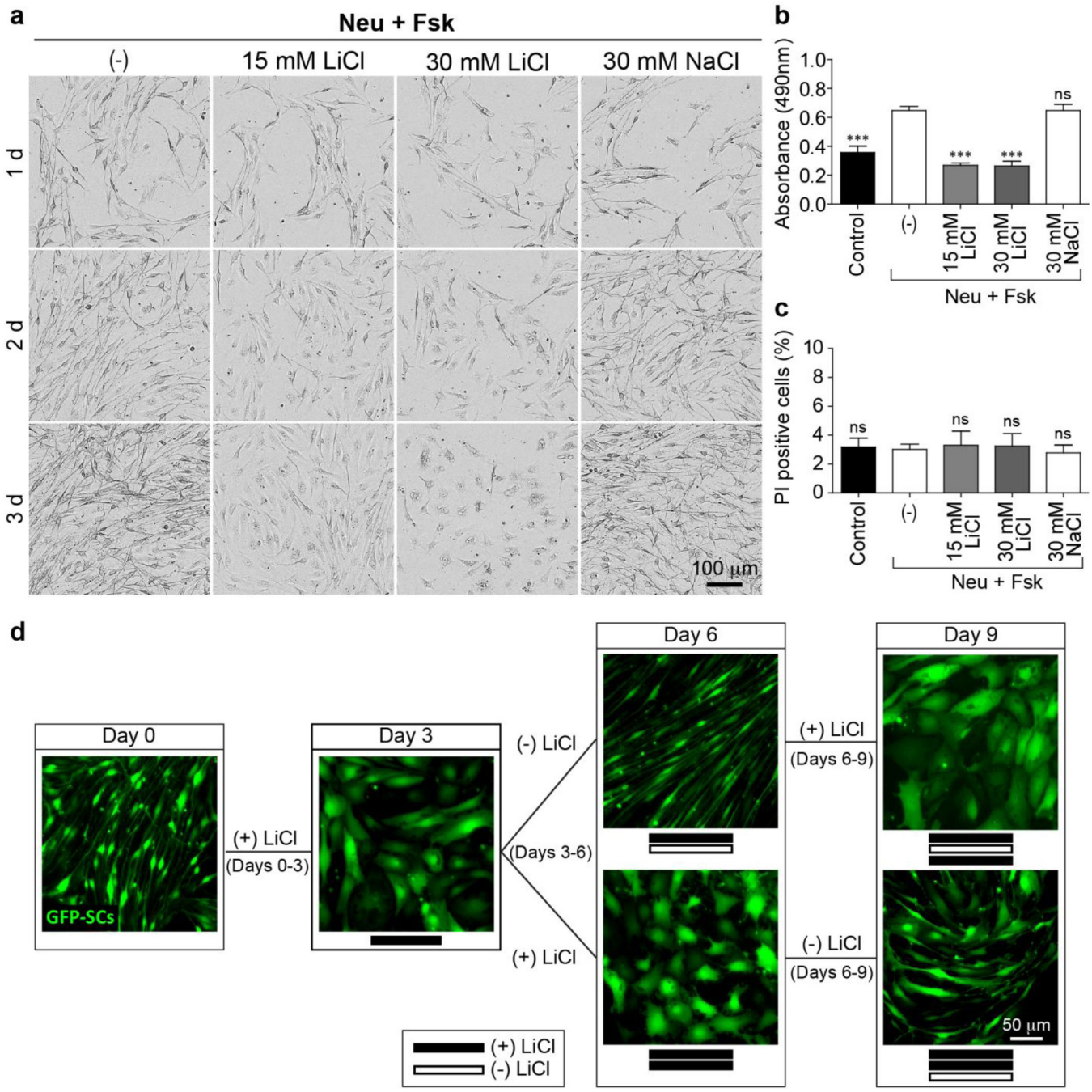

Fig. 2.

Lithium specifically and reversibly induces morphological changes without affecting cell survival, **a** Video-imaging of SC cultures treated with LiCl or NaCl in medium supportive of active proliferation. Neu (10 nM) and Fsk (2 µM) were administered in FBS-supplemented medium (control) in the absence or presence of LiCl or NaCl (as indicated). Selected areas were monitored over a time period of 3 days (3d) following the onset of treatment. Representative images of cells taken at the indicated time points are shown to represent the temporal increase in cell density that results from induction of proliferation (control) along

with the inhibitory effect of LiCl. Note that LiCl-treated SCs acquired a flattened, expanded morphology even in the presence of mitogenic factors. Morphological changes, including the appearance of intracellular vacuoles were more apparent with higher concentrations of LiCl. **b–c** Assessment of cell viability in lithium-treated cells. Experimental conditions were identical to those described in **a**. Cultures were analyzed 3 days after treatment by means of MTS assays (**b**) and PI incorporation assays (**c**). The proportion of PI positive cells was calculated with respect to the total number of cells labelled with Hoechst. No apparent changes in cell viability in response to LiCl or NaCl were observed during the course of these experiments. Bar graphs are represented as the mean ±SEM. Statistical analysis was done through repeated measures one-way ANOVA, followed by Dunnett's post-test. SCs treated with Neu and Fsk in the absence of LiCl were selected as control in the post-test. Statistical significance in all figures was annotated as follows: ns = not significant; * = $p < 0.05$; ** $p < 0.01$; *** = $p < 0.001$. **d** Recovery of a spindle-shaped morphology after LiCl withdrawal. Lentivirally-infected SCs (GFP-SCs) were subjected to repeated 3-day cycles of LiCl addition (black rectangles, 30 mM) and LiCl removal (white rectangles, vehicle). Cells were maintained in DMEM medium containing 10% FBS throughout the time course of the experiment to support cell survival over a prolonged period of time (9 days). Images of GFP fluorescence were taken at the indicated time points (i.e. 3, 6 and 9 days after treatment initiation). Note that SCs acquire a flattened and expanded (vacuolated) cytoplasm in the presence of LiCl and a spindle-shaped, elongated morphology in the absence of LiCl regardless of previous treatment.

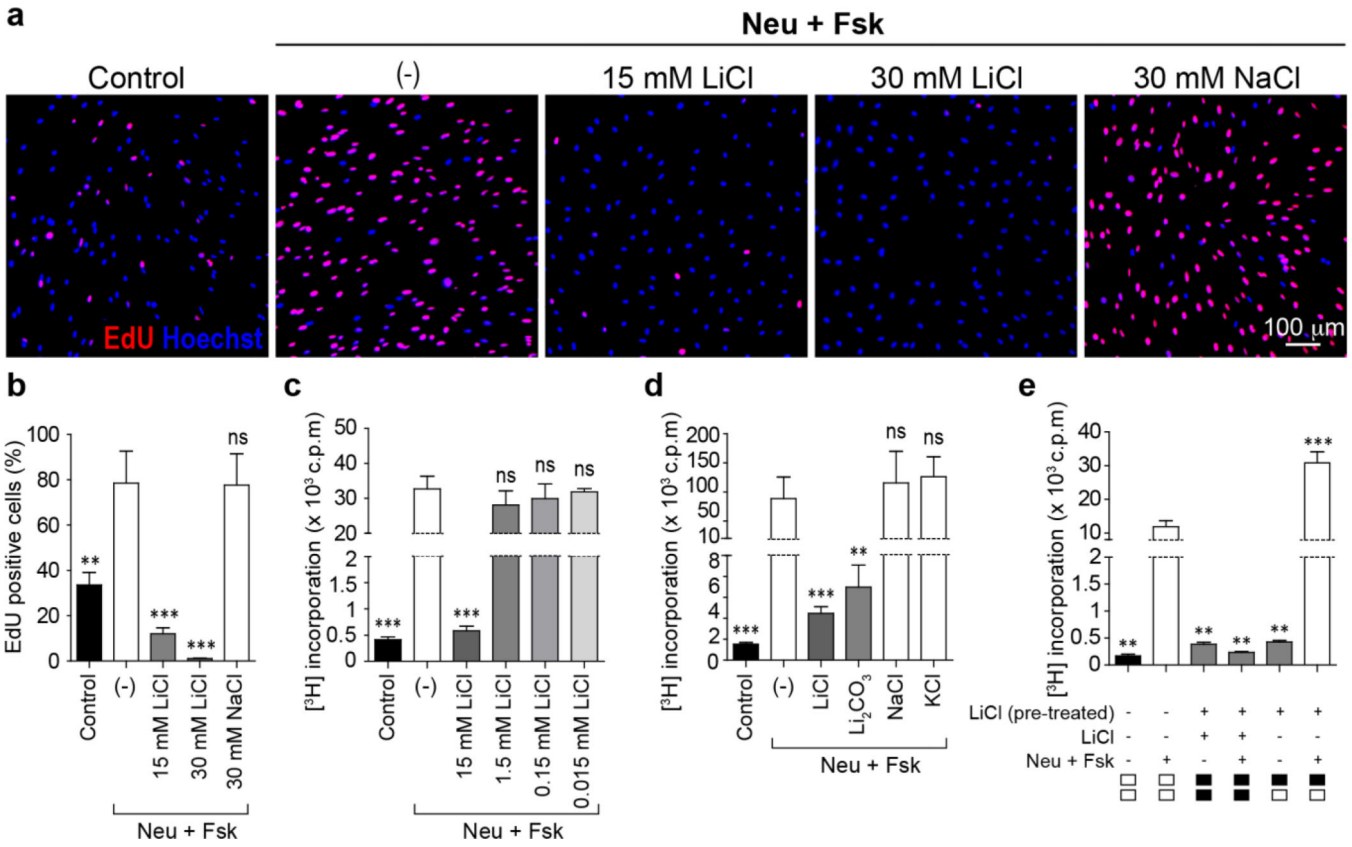

Fig. 3.

Lithium specifically, dose dependently and reversibly prevents mitogen-induced DNA synthesis in cultured isolated SCs, **a–b** Inhibitory effect of LiCl on mitogen-induced EdU incorporation. Representative images of EdU labeling (**a**) are shown along with a quantitative analysis of the image data (**b**). Cells were treated for 3 days with LiCl or NaCl in medium containing 10% FBS together with Neu and Fsk, as indicated. Medium containing 10% FBS was used as control. **c–d** Dose dependency and specificity of lithium's inhibitory effect on [^{3}H]-thymidine incorporation. Cultures were treated as described in panel **a** with the exception of the use of [^{3}H]-thymidine instead of EdU to label the nuclei of proliferating cells. The concentrations of LiCl used in panel **c** are indicated in the figure. In panel **d**, equimolar doses of LiCl (30 mM), Li_2CO_3 (15 mM), NaCl (30 mM) and KCl (30 mM) were provided. Li_2CO_3 is a clinically relevant lithium compound utilized to validate LiCl's activity and specificity of action in cultured SCs. **e** Recovery of proliferative capacity after LiCl withdrawal. SCs were pre-treated for 3 days in the presence of 30 mM LiCl (black rectangles). Subsequently, the medium was removed and replaced by new medium containing (black rectangles) or lacking (white rectangles) LiCl in the absence or presence of Neu and Fsk, as indicated. Notice the significantly higher levels of SC proliferation in response to mitogens (Neu + Fsk) detected in cells receiving LiCl-pretreatment. Bar graphs are represented as the mean ±SEM. Statistical analysis was done through repeated measures one-way ANOVA, followed by Dunnett's post-test. The condition of Neu and Fsk without LiCl was used as control in the post-test. Statistical significance in all figures was annotated as follows: ns = not significant; * = $p < 0.05$; ** $p < 0.01$; *** = $p < 0.001$.

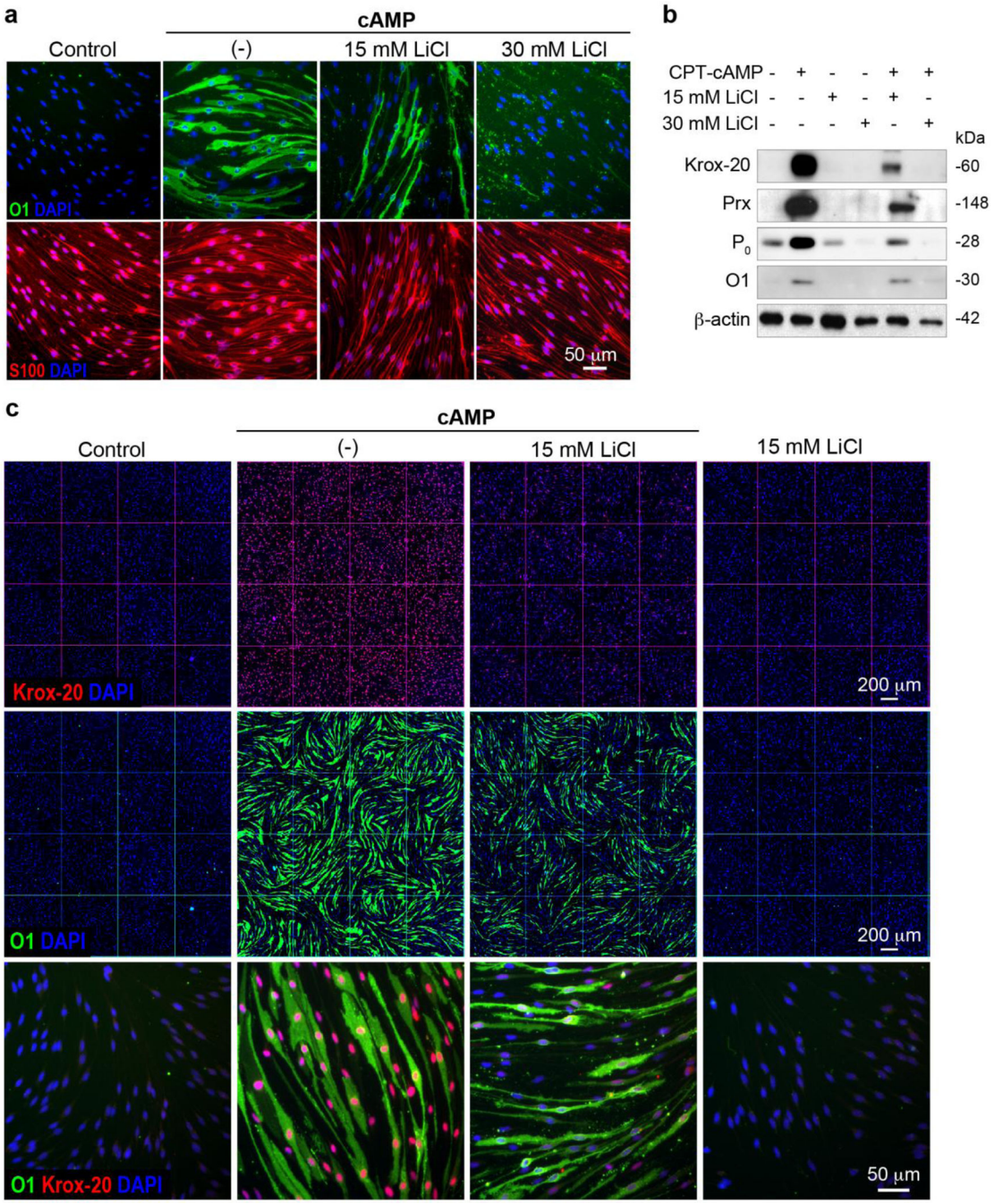

Fig. 4.

Lithium prevented the morphological changes and the induction of the expression of myelinating SC markers in response to cAMP, Mitogen-deprived SCs were treated with cAMP (250 μM) with or without the indicated concentrations of LiCl. Non-treated cells (control, vehicle) and cells solely treated with LiCl were included for reference purposes. All treatments were performed in DMEM containing 10% FBS to maintain cell viability throughout the time course of treatment. The expression of the indicated markers at day 4 post-stimulation was determined by immunofluorescence microscopy (**a** and **c**) and western

blot analysis (**b**). A panoramic, low magnification view of cultures double-immunostained with O1 (green) and Krox-20 (red) antibodies is shown to highlight the magnitude of the antagonistic effect of LiCl on cAMP-driven differentiation (**c**, upper and middle panels). Note that a concentration of 30 mM LiCl was sufficient to abrogate the cAMP-induced expression of Krox-20, P_0, Prx and O1 (**a-b**).

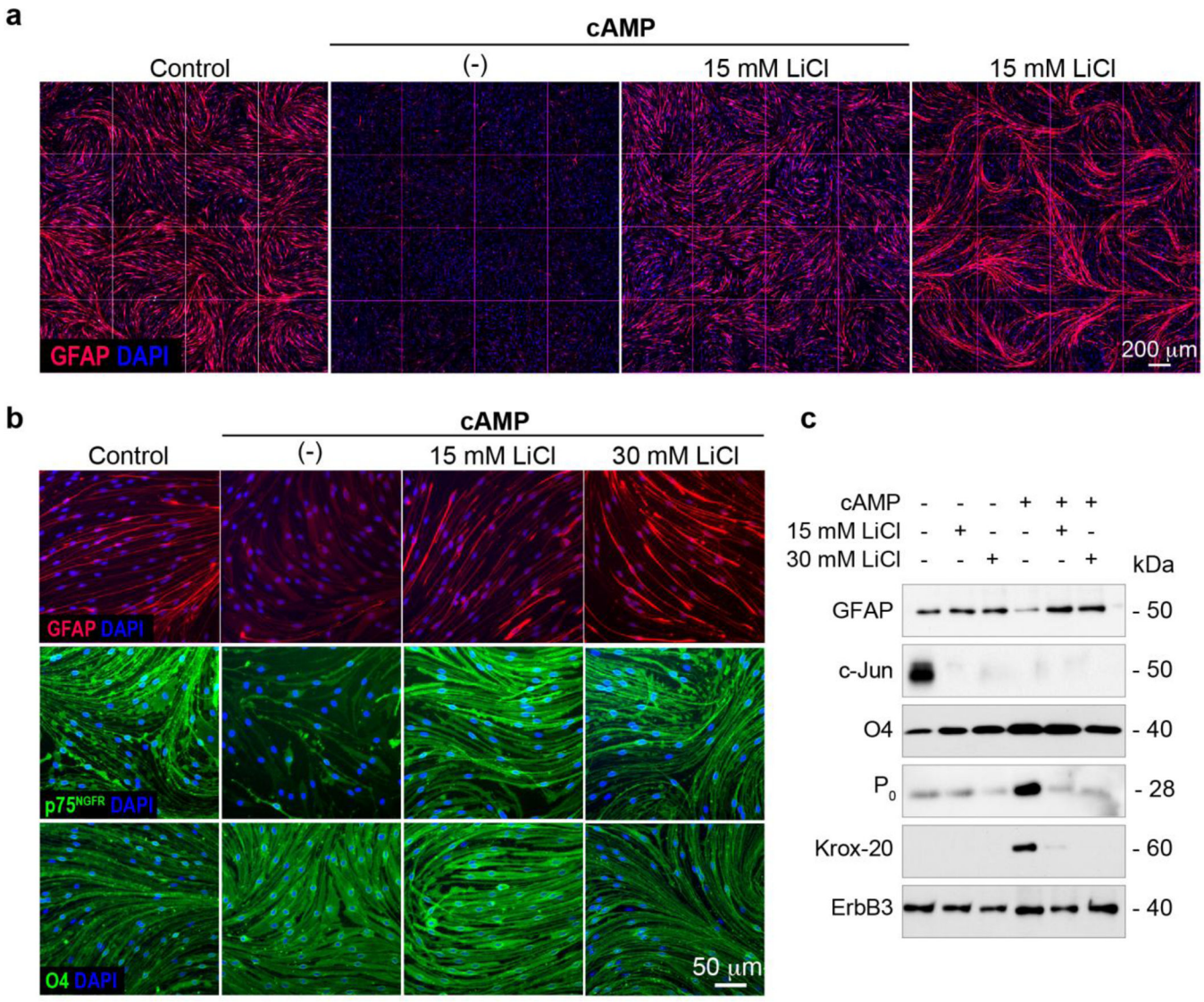

Fig. 5.

Lithium reduces c-Jun expression while maintaining high levels of GFAP and $p75^{NGFR}$ in the presence of differentiating doses of cAMP, Experiments were carried out and analyzed essentially as described in Fig. 4. Mitogen-deprived SCs were treated with cAMP (250 μM) with or without LiCl (30 mM) and the levels of expression of the indicated markers were determined by fluorescence microscopy (**a-b**) and western blot analysis (**c**) 4 days after the onset of treatment. Panel **c** depicts the relative expression profiles of various markers (as indicated) in samples collected in parallel experiments. The expression of ErbB3 was used as a control for total SC protein. In **a**, a panoramic view of cultures stained with GFAP antibodies is shown to illustrate the magnitude of the changes induced by cAMP alone and together with LiCl in the overall SC population. Similar to cAMP, treatment of SC cultures with LiCl alone was sufficient to abrogate c-Jun expression (**c**). As opposed to cAMP, blockage of c-Jun expression by lithium occurred without a concurrent increase in the expression of myelinating SC markers (shown in panel **c** for Krox-20 and P_0) or a reduction

in the expression of GFAP and $p75^{NGFR}$ (shown in panels **a-c**). As a control, note that LiCl did not reduce the levels of expression of cell surface O4 (**b-c**) or ErbB3 (**c**) when given in combination with cAMP.

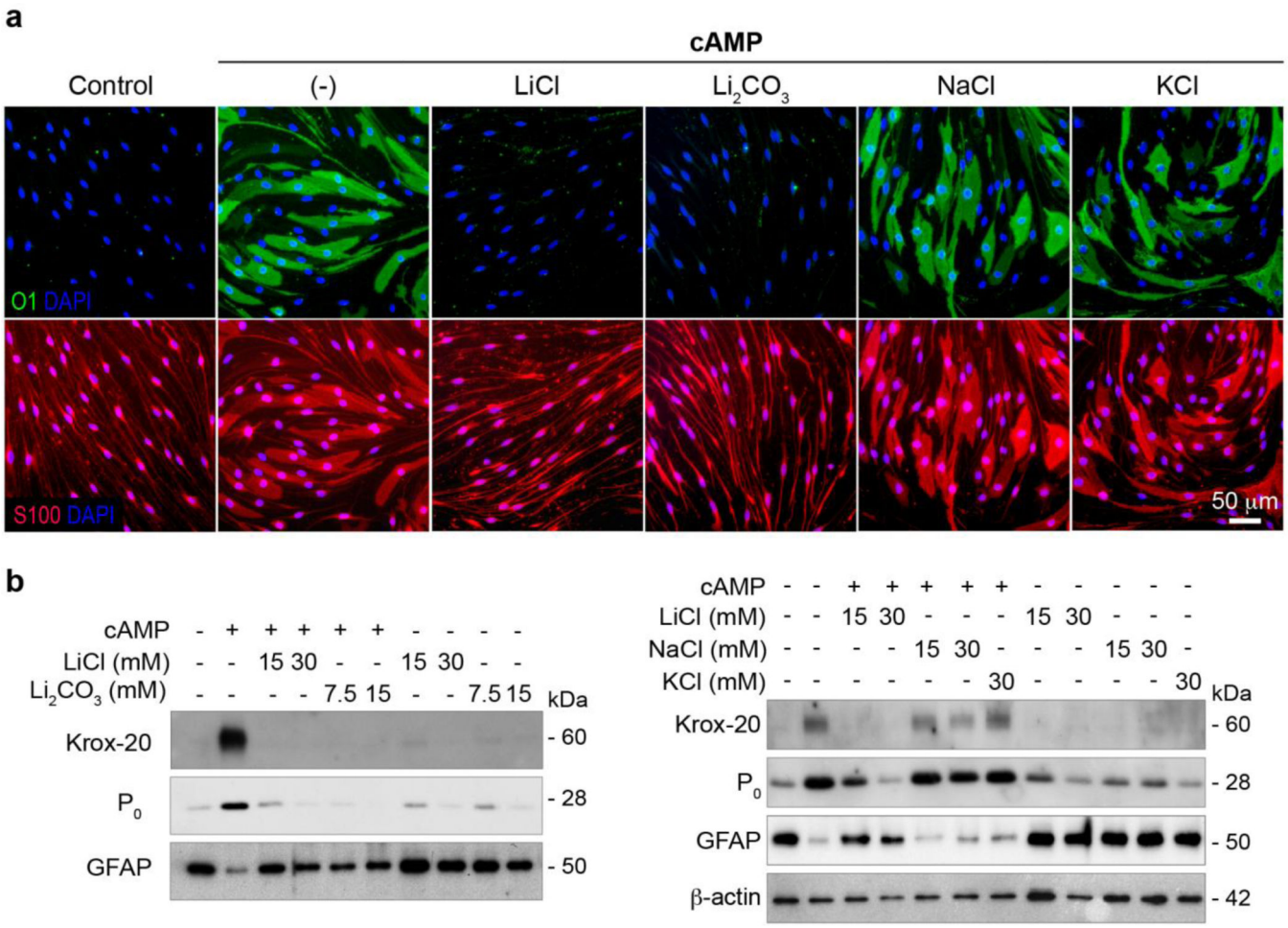

Fig. 6.

Specificity of lithium's inhibition of cAMP-induced SC differentiation, Mitogen-deprived SCs were treated with cAMP (250 µM) alone or in conjunction with an equimolar concentration of LiCl (15, 30mM), Li_2CO_3 (7.5, 15 mM), NaCl (15, 30 mM) and KCl (30 mM) for 3 days. Non-treated cells (vehicle) were used as controls for non-differentiated cells. Sister cultures were processed for analysis by immunofluorescence microscopy (**a**) and western blot (**b**) using the antibodies indicated in the figure. Note that NaCl and KCl were not able to block the expression of Krox-20, P_0 and O1, under conditions supportive of differentiation. In panel **a**, selected areas of cultures double-immunostained with 01 (green) and S100 (red) antibodies are provided to show that the reduction in O1 expression occur while maintaining high levels of expression of S100.

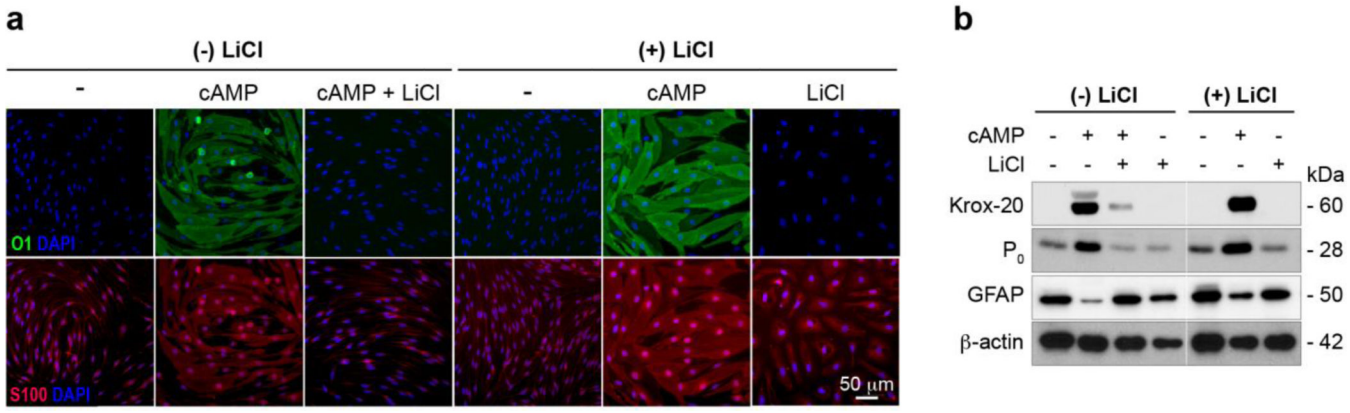

Fig. 7.

Reversibility of lithium's inhibition of cAMP-induced SC differentiation, Cultured SCs were left untreated [(−) LiCl] or treated with LiCl for 3 days [(+) LiCl] prior to administering cAMP in the absence or presence of freshly added LiCl (30 mM). Cells were analyzed by immunofluorescence microscopy (**a**) or western blot (**b**) 3 days after provision of cAMP (250 μM), essentially as described in previous figures. In **a**, cultures double-immunostained with O1 (green) and S100 (red) antibodies are provided to reveal the changes in cell shape and size in each experimental condition.

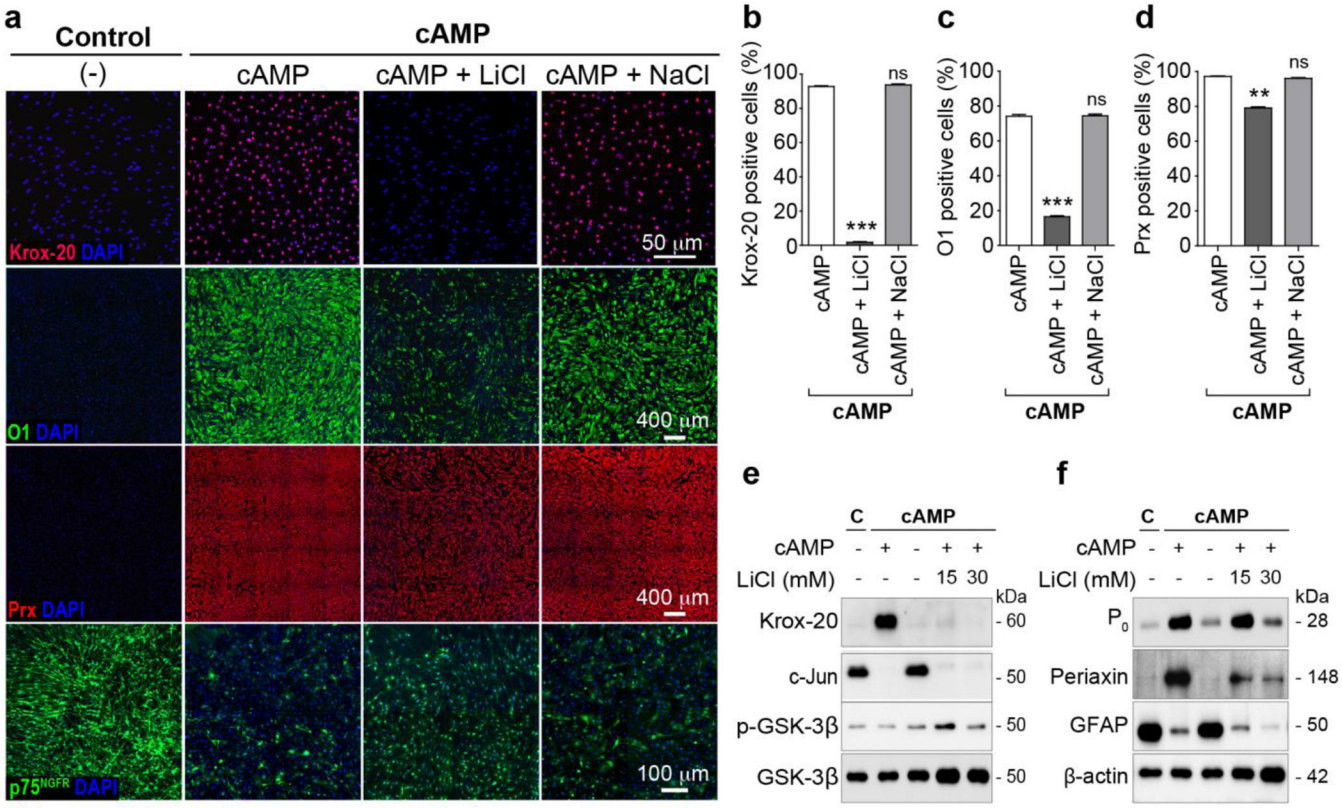

Fig. 8.

Lithium specifically reduces Krox-20 expression in cAMP-differentiated SCs without driving the expression of c-Jun, GFAP and $p75^{NGFR}$, Isolated SCs were treated with cAMP (250 µM) for 3 days prior to receiving treatment with LiCl (as indicated) in the presence of freshly added cAMP. In panels **a-d**, SCs were treated with NaCl (30 mM) as a specificity control. In panels **e** and **f**, cAMP was removed from the culture medium to promote the reactivation of immature SC markers [31]. Non-treated cells (vehicle) were used as controls throughout [(−) cAMP, in panels **e** and **f**]. Cultures were processed for analysis by immunofluorescence microscopy (**a-d**) and western blot (**e** and **f**) 3 days after the removal of cAMP or provision LiCl/NaCl (in the presence of cAMP). Whereas LiCl abolished Krox-20 expression, it only partially reduced the expression of O1 (**d, e**) and Prx (**d**, **f**) under the same experimental conditions. Note that LiCl rather than NaCl interferes with the expression of Krox-20 (**a-b**) without allowing cells to regain high levels of expression of c-Jun (**e**), GFAP (**f**) and $p75^{NGFR}$ (**a**). Bar graphs shown in **b–d** are represented as the mean ±SEM. Statistical analysis was done through repeated measures one-way ANOVA, followed by Dunnett's post-test. Statistical significance was annotated as follows: ns = not significant; * = $p < 0.05$; ** $p < 0.01$; *** = $p < 0.001$. In panel **e**, the profiles of phosphorylated and total GSK-3β are shown to confirm the bioactivity of LiCl in cAMP-differentiated SCs.

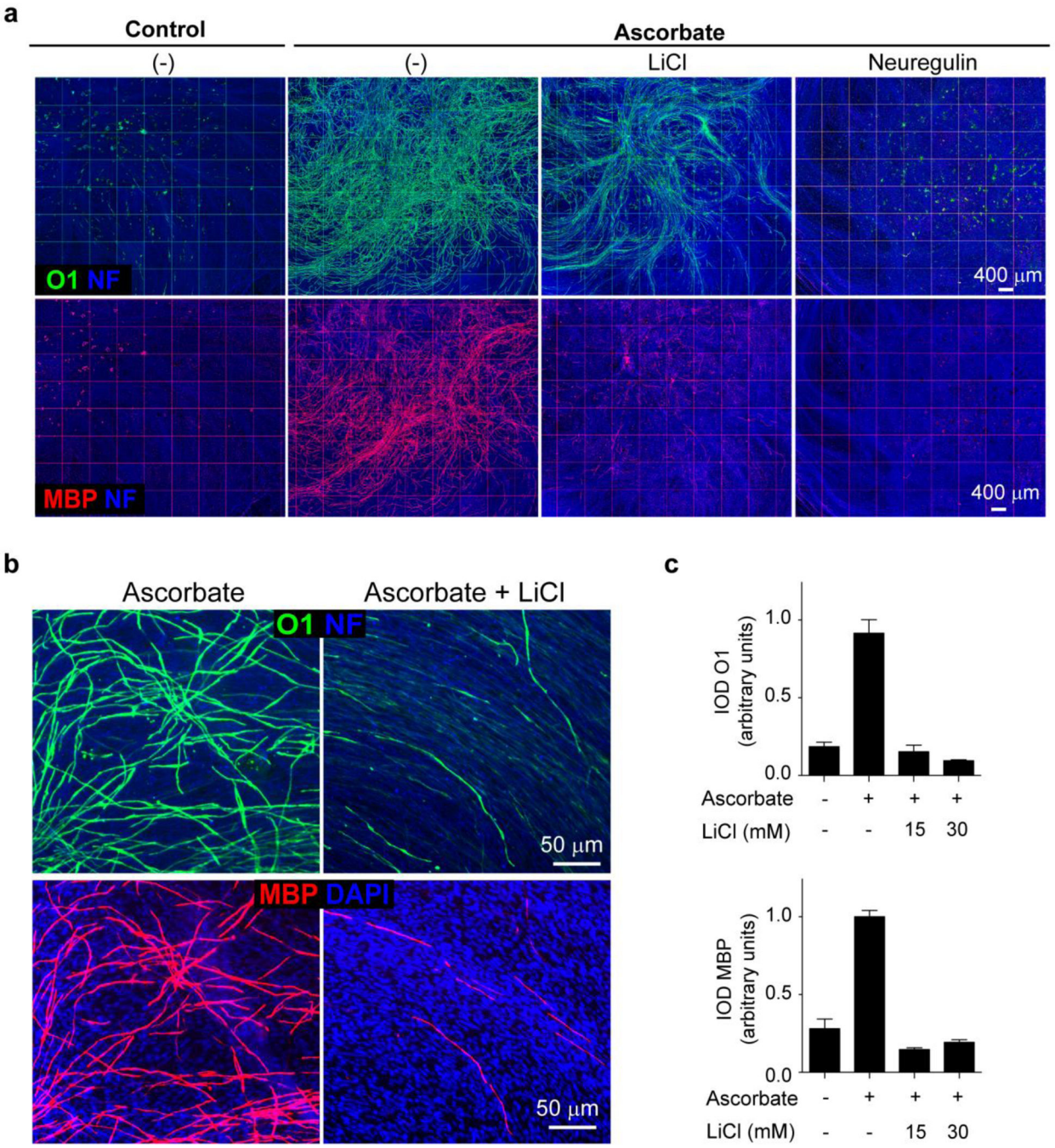

Fig. 9.

Lithium prevents myelin formation in ascorbate-treated SC-neuron cultures, SCs co-cultured with DRG neurons (standard methods) were induced to form myelin by the addition of L-ascorbic acid (ascorbate) in the absence (control, vehicle) or presence of LiCl (7 mM unless otherwise noted) or Neu (50 nM). These agents were maintained in the culture medium throughout the time course of the experiments (7 days). Fresh LiCl or Neu were incorporated in the culture medium used for re-feeding every other day after the onset of treatment (methods). In panels **a-b**, myelin sheaths were visualized by co-immunostaining

using MBP (red) and O1 (green) antibodies. A quantification of IOD for O1 and MBP is shown in **c**. Bar graphs are represented as the mean ±SEM, normalized to the IOD value obtained in the ascorbate condition. Axons were visualized by staining with NF antibodies (blue) in all images. Nuclei were counterstained with DAPI (panel **b**, blue). Images of myelinating co-cultures are presented at low (**a**, panoramic view) and high magnification (**b**) to reveal the relative density and quality of the myelin sheaths, respectively. Inhibition of MBP expression in response to LiCl was typically more pronounced than that seen for O1, as suggested by the lesser density (**a**) and thinner profiles (**b**) of MBP immunostaining. Higher concentrations of LiCl (15–30 mM) nearly abolished O1 and MBP expression (**c**), resembling the action of soluble Neu.

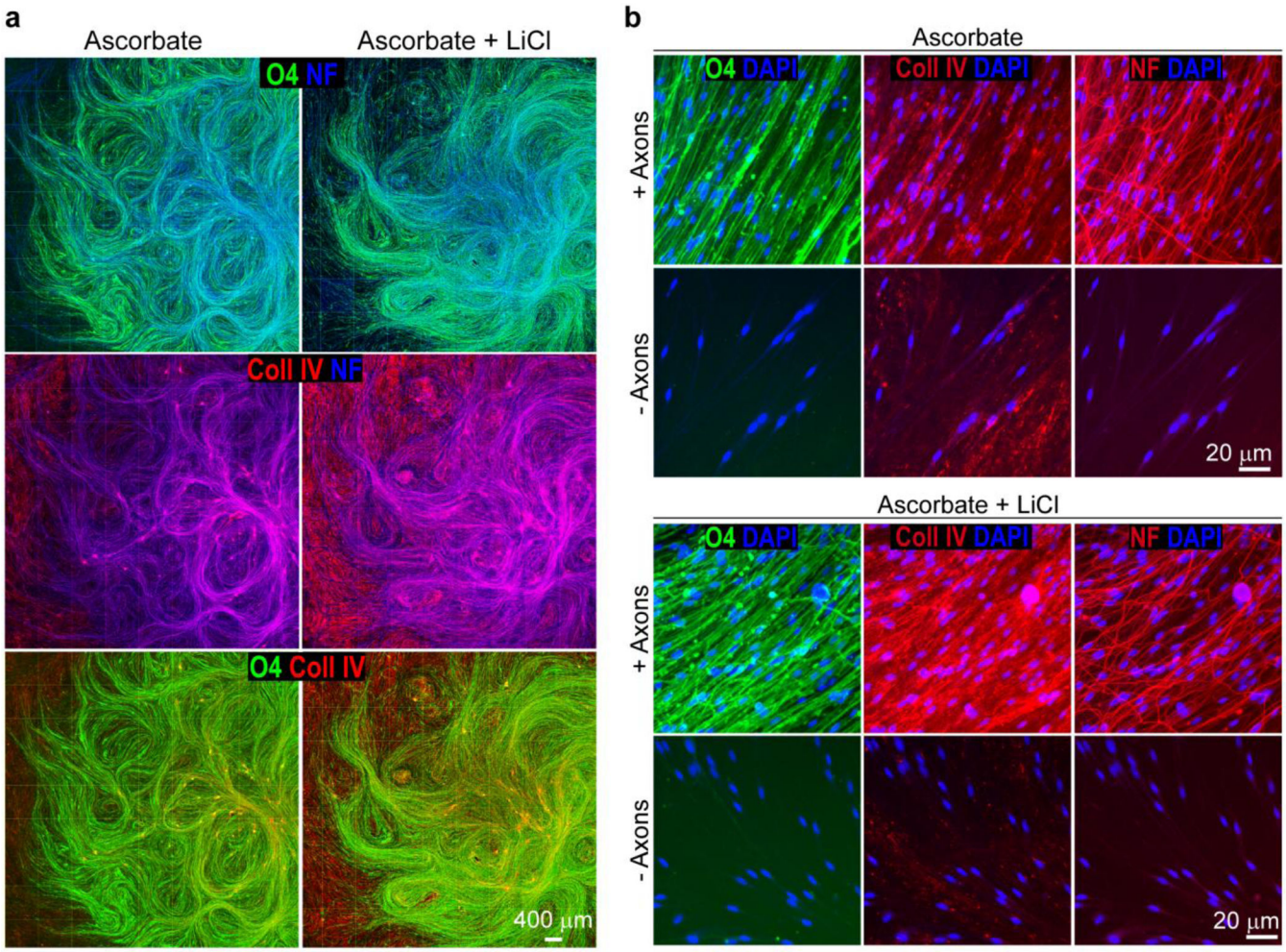

Fig. 10.

Lithium does not impair axon-induced O4 and collagen type IV expression in ascorbate-treated SC-neuron cultures, SC-DRG neuron cultures were prepared and stimulated with LiCl (15 mM), essentially as described in Fig. 9, with the exception that axon-related SCs (non-myelinating and myelinating) were identified by live cell immunostaining with O4 antibodies (green). ECM formation was revealed by immunostaining with collagen type IV antibodies (Coll IV, red) in the same cultures. Axons were visualized by staining with NF antibodies (blue channel in a, red channel in b) and nuclei were counterstained with DAPI (shown only in panel **b**). Images from representative cultures are presented at low (**a**, panoramic view) and high magnification (**b**). In **b**, selected areas within (+ axons) and outside (− axons) the axonal outgrowth (NF) are shown to reveal the changes in O4 and collagen IV expression in axon-related (+axons) and axon-deprived (−axon) SCs, respectively. As expected, SCs located outside the neuronal network (periphery of the culture) were negative for O4 expression under our experimental conditions. Cell surface staining with O4 antibodies provided no evidence of impaired SC alignment to axons in LiCl-treated cultures (**b**).

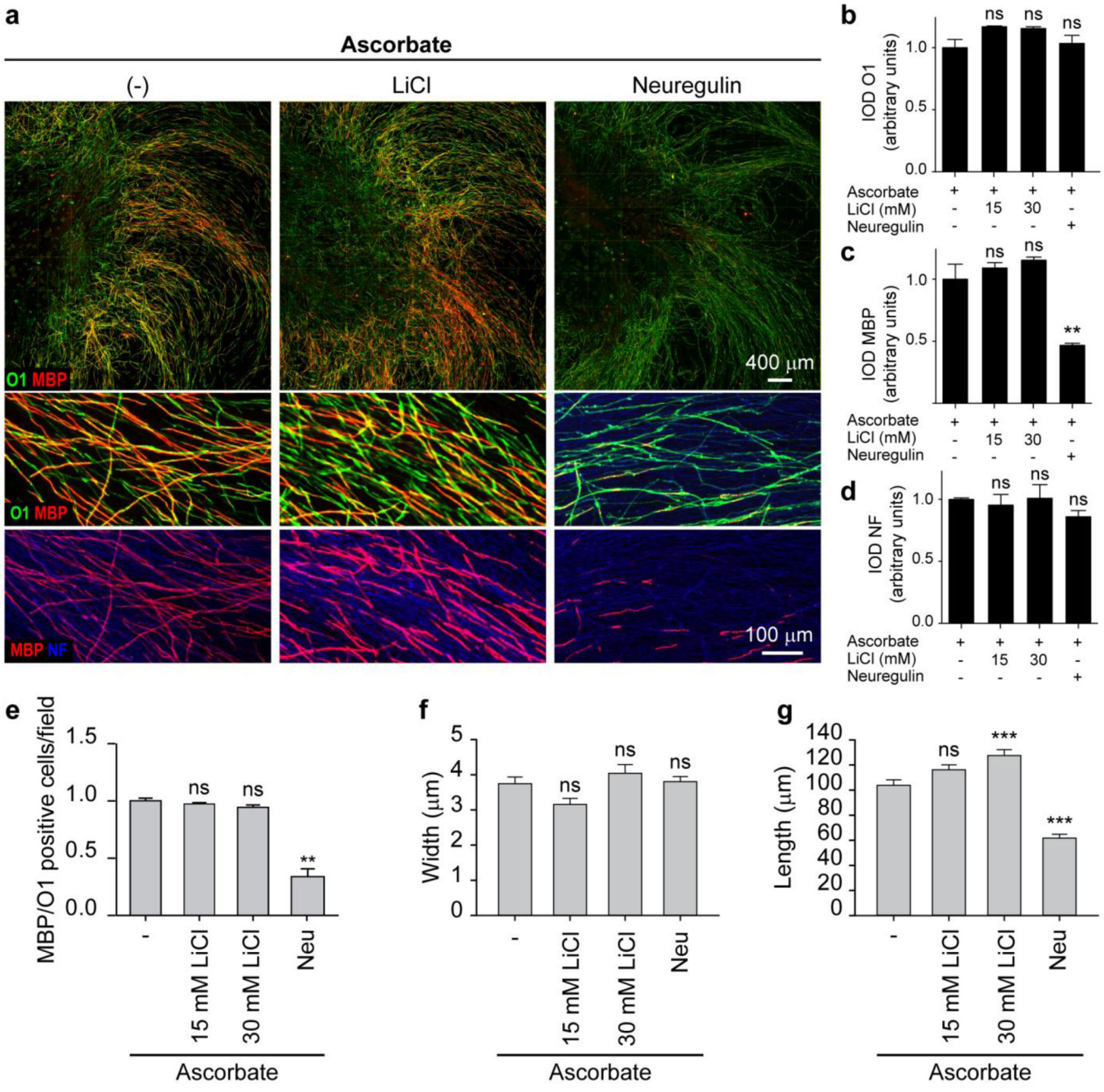

Fig. 11.

Lithium preserves the integrity of pre-existing myelinated fibers, **a** Representative immunofluorescence microscopy images of myelinating SC-neuron cultures treated with LiCl or Neu. **b–d** Quantification of the relative levels of O1, MBP and NF expression over a large surface area based on fluorescence microscopy data. **e** Quantification of the number of myelin sheaths in selected areas outside of the area containing the neuronal bodies (MBP positive /O1 positive cells). **f, g** Morphometric analysis of MBP positive myelin segments. SC-DRG neuron cultures were induced to form myelin by the addition of L-ascorbic acid (ascorbate) for 7 days (as described in Fig. 9) followed by treatment with vehicle (control),

LiCl (30 mM or as indicated) or Neu (50 nM) for an additional 2-day period. Myelin sheaths, axons and nuclei were identified as described in Fig. 9. In panel **a**, representative images taken at low (upper panels) and high (lower panels) magnification were selected to show the effect of high doses of LiCl and Neu on myelin quantity and quality, respectively (see Methods). LiCl not only failed to mimic the demyelinating effect of Neu but also moderately enhanced O1 and MBP expression throughout the culture area (**a-c**). Compare the appearance of intact myelinating SCs (**a**, left and middle panels) with that of Neu-treated SCs (**a**, right panel). In the Neu group, de-differentiating SCs exhibited long, highly branched processes which stained positive for O1 (**a**, lower panels). No evident cytotoxic effects of LiCl were observed on SCs or neurons under these conditions. Axonal integrity was preserved in all conditions as revealed by staining with NF (**a** and **d**). Myelin fragmentation or other signs of SC dedifferentiation were not observed in control or LiCl-treated cultures. Bar graphs are represented as the mean ±SEM; in **b–d** and **e**, data was normalized to the ascorbate condition. Statistical analysis was done through repeated measures one-way ANOVA, followed by Dunnett's post-test. Statistical significance was annotated as follows: ns = not significant; * = $p < 0.05$; ** $p < 0.01$; *** = $p < 0.001$.